

## Metalloocene-Based Inhibitors of Cancer-Associated Carbonic Anhydrase Enzymes IX and XII

Adam J. Salmon,<sup>†</sup> Michael L. Williams,<sup>†</sup> Quoc K. Wu,<sup>‡</sup> Julia Morizzi,<sup>‡</sup> Daniel Gregg,<sup>‡</sup> Susan A. Charman,<sup>‡</sup> Daniela Vullo,<sup>§</sup> Claudiu T. Supuran,<sup>\*,§</sup> and Sally-Ann Poulsen<sup>\*,†</sup>

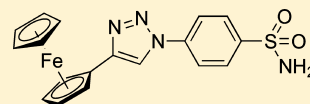
<sup>†</sup>Eskitis Institute for Cell and Molecular Therapies, Griffith University, Nathan, Queensland 4111, Australia

<sup>‡</sup>Centre for Drug Candidate Optimisation, Monash Institute of Pharmaceutical Sciences, Monash University (Parkville Campus), 381 Royal Parade, Parkville, Victoria 3052, Australia

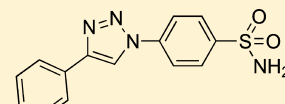
<sup>§</sup>Polo Scientifico, Laboratorio di Chimica Bioinorganica, Rm. 188, Università degli Studi di Firenze, Via della Lastruccia 3, 50019 Sesto Fiorentino, Florence, Italy

### S Supporting Information

**ABSTRACT:** In this study, 20 metalloocene-based compounds comprising extensive structural diversity were synthesized and evaluated as carbonic anhydrase (CA, EC 4.2.1.1) inhibitors. These compounds proved moderate to good CA inhibitors in vitro, with several compounds displaying selectivity for cancer-associated isozymes CA IX and CA XII compared to off-target CA I and CA II. Compound **6** was the most potent ferrocene-based inhibitor with  $K_i$ s of 5.9 and 6.8 nM at CA IX and XII, respectively. A selection of key drug-like parameters comprising Log *P*, Log *D*, solubility, and in vitro metabolic stability and permeability were measured for two of the ferrocene-based compounds, regioisomers **1** and **5**. Compounds **1** and **5** were found to have characteristics consistent with lipophilic compounds, however, our findings show that the lipophilicity of the ferrocene moiety is not well modeled by replacement with either a naphthyl or a phenyl moiety in software prediction tools.



CA II  $K_i$  = 80 nM  
 CA IX  $K_i$  = 85 nM  
 Log  $D_{7.4}$  = 2.9  
 $P_{app}$  =  $5.8 \times 10^{-5}$  cm/s  
 Equil. Solubility = 1.7  $\mu$ g/mL



CA II  $K_i$  = 47 nM  
 CA IX  $K_i$  = 72 nM  
 Log  $D_{7.4}$  = 2.3  
 $P_{app}$  =  $5.8 \times 10^{-5}$  cm/s  
 Equil. Solubility = 1.4  $\mu$ g/mL

### INTRODUCTION

Reports of safe and efficacious organometallic inhibitors for a growing number of therapeutically relevant enzymes have resulted in widened acceptance of organometallic compounds as viable candidates for targeted therapeutic applications.<sup>1</sup> To date, numerous classes of organometallic compounds have found application in medicinal chemistry; these include metallocenes, half-sandwich metallocenes, metal carbenes, metal carbonyls, and metal-arene compounds.<sup>1</sup> The classical metallocenes, ferrocene and ruthenocene, are sandwich compounds wherein the metal is located between two cyclopentadienyl (Cp) rings. These compounds are stable in air, kinetically inert, and uncharged, with their metal atom in a low oxidation state. Both ferrocene and ruthenocene are amenable to derivatization reactions such as Friedel-Craft acylations, formylation, sulfonation, and lithiation (to name a few), and this permits a straightforward synthesis of metalloocene-based organometallic compounds.<sup>2</sup> The toxicology of ferrocene is particularly well studied, and this compound may be administered orally without toxicity.<sup>3</sup> Ferrocene is metabolized in the liver by cytochrome P450 enzymes similarly to benzenes.<sup>3</sup> Ferrocenium salts were the first organometallic compounds for which antiproliferative properties were reported,<sup>4</sup> and today there are a number of ferrocene-based compounds that have found use as therapies.<sup>3</sup> Notably, the replacement of a benzene ring with a ferrocene fragment within

the structure of two established drugs has led to compounds wherein the ferrocene chemistry is implicated in the drug mode of action. Hydroxyferrocifen is a ferrocene analogue of tamoxifen that selectively targets breast cancer,<sup>5</sup> while ferroquine is a ferrocene analogue of chloroquine that targets the malaria parasite; both of these ferrocene analogues are in clinical development.<sup>6</sup> An alternate approach, wherein the ferrocene moiety is appended as a substituent onto a known pharmacophore, has been applied in a number of successful medicinal chemistry campaigns to take advantage of the physicochemical and structural properties of ferrocene for improved biological activity.<sup>3</sup> Ruthenocene and its derivatives are much less studied than their isostructural ferrocenyl counterparts, and to date only a small number of ruthenocene-based compounds appear in the literature in the context of drug discovery.<sup>7</sup>

Carbonic anhydrases (CAs) are zinc metalloenzymes that catalyze the reversible hydration of carbon dioxide to bicarbonate and a proton.<sup>8</sup> CA isozymes IX and XII are overexpressed in cancer cells of many hypoxic tumors where they provide a pH-regulating system that contributes to hypoxic tumor cell survival and proliferation.<sup>9</sup> The significance of CAs role in cancer has triggered a need to develop novel, drug-like

Received: March 26, 2012

Published: April 27, 2012

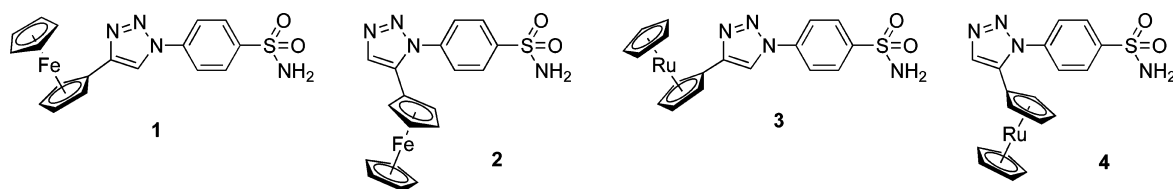


Figure 1. Metallocene-based CA inhibitors 1–4 synthesized by 1,3-DCR.

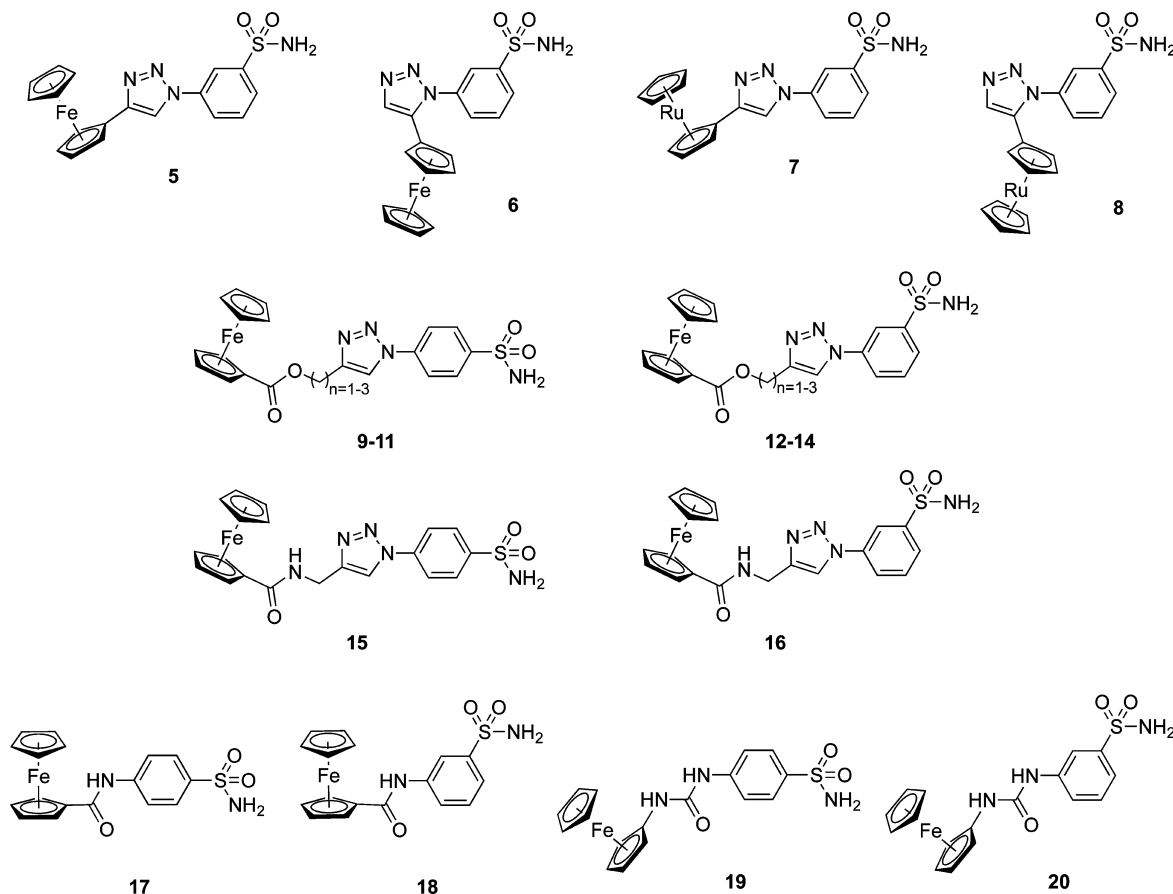


Figure 2. Novel metallocene-based CA inhibitors 5–20.

small molecule CA inhibitors as chemical tools and/or as leads for therapeutic drug discovery.<sup>10</sup> Small molecule CA inhibitors have recently been reported that show promising anticancer properties.<sup>11</sup> In this article, we report the design, synthesis, biological activity, and selected ADME properties for a library of novel metallocene-based CA inhibitors. The development of metallocene-based compounds that can selectively kill tumor cells by inhibiting the validated oncology target CA IX is a new approach with potential to deliver organometallic, drug-like compounds as future therapies. We recently reported the protein X-ray crystal structures of four of these compounds in complex with CA II (PDB accession codes 3P55, 3P3H, 3P44, and 3P3J),<sup>12</sup> while others have recently reported structures of piano-stool complexes bound to CA II.<sup>13</sup> Our study is the first wherein isomeric ruthenocene and ferrocene inhibitors have been complexed with the target protein and a crystal structure obtained.<sup>12</sup> The replacement of ferrocene (iron) with ruthenocene (ruthenium) altered the CA enzyme inhibition of these compounds in a manner consistent with the subtle but significant difference in structure provided by changing the metal. We demonstrated that although the metallocene moiety

behaves chemically like an aromatic moiety such as a phenyl group,<sup>7a</sup> the barrel-shaped sandwich structure of the metallocene fragment permits access to 3D structural permutations that are not possible with a flat aromatic ring.<sup>12</sup> We identified several hydrophobic interactions with the hydrophobic face of the CA II binding cavity and hypothesized that this may provide an avenue to continue to develop new metallocene-based compounds that better occupy the hydrophobic binding pocket of CAs active site to further inform structure–activity relationships (SAR) of this organometallic class of CA inhibitors.

## RESULTS AND DISCUSSION

**Inhibitor Design.** The “tail approach” has been applied to the design and synthesis of a growing number of potent and isozyme selective CA inhibitors. The approach involves covalently tethering a tail fragment onto the established primary sulfonamide CA recognition pharmacophore (R-SO<sub>2</sub>NH<sub>2</sub> where R = aromatic) to generate the extended pharmacophore: [tail]–[aromatic]–[ZBG].<sup>14</sup> The approach has provided a framework in which CA inhibitor properties can

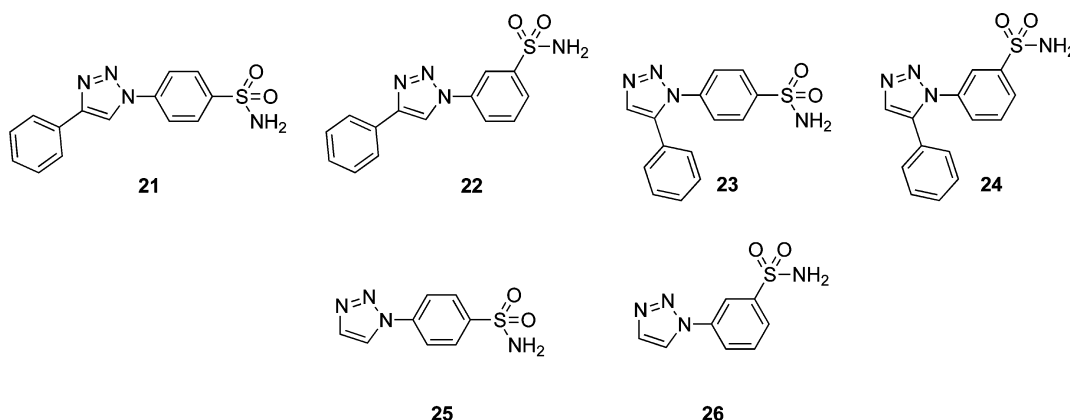


**Figure 3.** Control compounds in which the triazole-metallophenyl tail fragment is replaced by a triazole-phenyl tail fragment (21–24) or an unsubstituted triazole tail fragment (25, 26).

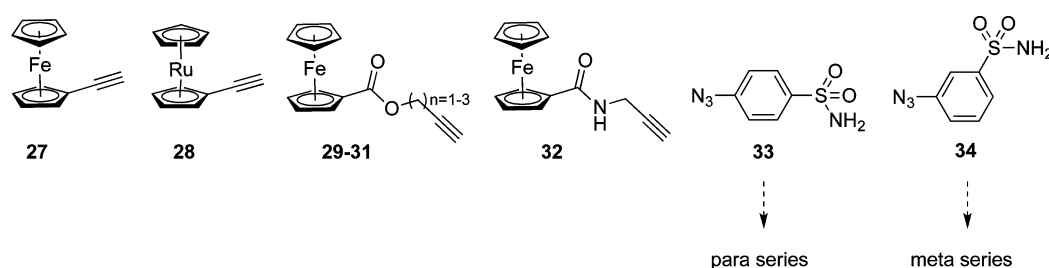
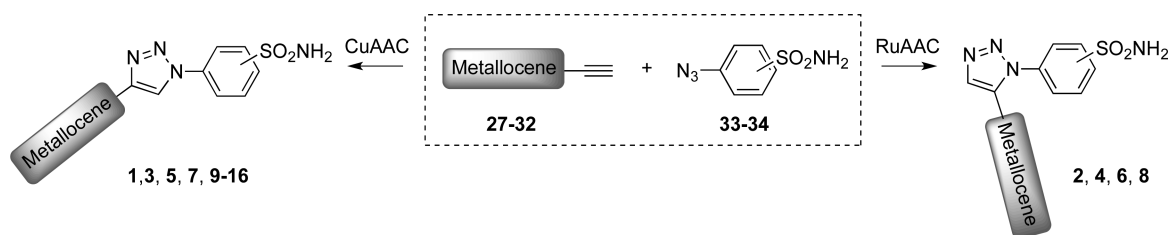


**Figure 4.** Metallocene-based alkynes (27–32) and [aromatic]-[ZBG] azide (33 and 34) building blocks.

### Scheme 1. Synthesis of Metallocene-Based CA Inhibitors 1–16 Using Either CuAAC or RuAAC<sup>a</sup>



<sup>a</sup>Reagents and conditions. CuAAC: azide 33 or 34 (0.02–0.1 M), alkyne 27–32 (1.0 equiv),  $\text{CuSO}_4 \cdot 5\text{H}_2\text{O}$  (0.2 equiv), sodium ascorbate (0.4 equiv),  $t\text{BuOH}:\text{H}_2\text{O}$  (1:1), 40 °C, 18 h. RuAAC: azide 33 or 34 (0.02–0.15 M), alkyne 27 or 28 (1.0 equiv),  $[\text{Cp}^*\text{RuCl}(\text{PPh}_3)_2]$  or  $[\text{Cp}^*\text{RuCl}(\text{cod})]$  (5 mol %), toluene,  $\text{N}_2$ , 100 °C, 18 h.

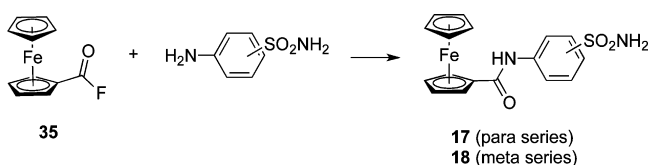
be readily tuned with respect to structure–property and structure–activity parameters to deliver CA inhibitors with biopharmaceutical characteristics that are appropriate for in vivo use. Commonly used covalent attachments between the aromatic group and tail fragment are ester, amide, imine, urea, and thiourea linkers. Previous work in our research group has focused on the 1,3-dipolar cycloaddition reaction (1,3-DCR) between alkynes and azides to generate novel CA inhibitors with triazole tails.<sup>15</sup> Using either 4-azido or 4-ethynyl benzene sulfonamide as the CA recognition pharmacophore and 1,3-DCR with a complementary alkyne or azide, we have synthesized compounds that comprise a tail fragment attached to a CA recognition pharmacophore through an intervening 1,2,3-triazole link.<sup>16</sup> We have previously presented the synthesis and CA enzyme inhibition of four metallocene-based CA inhibitors prepared by 1,3-DCR, compounds 1–4, Figure 1.<sup>7a</sup> These compounds comprise the [tail]–[aromatic]–[ZBG] extended pharmacophore, wherein a triazole–ferrocene or triazole–ruthenocene is the tail of the CA inhibitor. In the present study, we have synthesized 16 additional novel

metallocene-based CA inhibitors comprising more extensive structural diversity with attachment of the tail group, including triazole (5–8), triazole-ester (9–14), triazole-amide (15–16), amide (17–18), and urea (19–20) linkers, Figure 2. These linkers impart differing stability and hydrogen bonding attributes to these organometallic CA inhibitors. Compounds 1–20 comprise two isomeric series, the first series is the para-substituted benzene sulfonamide [aromatic]–[ZBG] series (1–4, 9–11, 15) and the second series is the meta-substituted benzene sulfonamide [aromatic]–[ZBG] series (5–8, 12–14, 16). In addition to metallocenes 1–20, six additional analogues were synthesized wherein the triazole–metallocene tail fragment was replaced with either a triazole–phenyl tail fragment (21–24) or an unsubstituted triazole fragment (25–26), Figure 3. Compounds 21–26 were designed as controls to allow delineation of the metallocene contribution to SAR and structure–property relationships (SPR).

**Chemistry.** The building blocks for the target compounds 1–20 comprise metallocene-based alkynes 27–32 and benzenesulfonamide azides 33 and 34, Figure 4. Metallocene-

based alkynes include ethynyl ferrocene **27**, ethynyl ruthenocene **28**, ethynyl ester substituted ferrocenes **29–31**, and ethynyl amide substituted ferrocene **32**. Compound **27** is commercially available, compound **28** was prepared as reported by us earlier,<sup>7a</sup> while esters and amide **29–32** were prepared from fluorocarbonylferrocene **35** and the respective alcohol or amine.<sup>17</sup> The acyl fluoride **35** is less susceptible to hydrolysis than the corresponding acyl chloride, and this permitted the straightforward handling, purification, and storage of **35**.<sup>17</sup> Azido benzenesulfonamides (**33**<sup>16d</sup> and **34**) were synthesized from their corresponding commercially available amines using neutral conditions reported for the synthesis of aryl azides.<sup>18</sup> Compound **34** is novel, and this is the first application of click chemistry from this azide. Compounds **1–16** were synthesized by 1,3-DCR of alkynes **27–32** with azides **33** and **34**. The 1,4-disubstituted-1,2,3-triazole inhibitors **1**, **3**, **5**, **7**, and **9–16** were synthesized by copper-catalyzed azide–alkyne cycloaddition (CuAAC), while the 1,5-disubstituted-1,2,3-triazole regioisomers **2**, **4**, **6**, and **8** were synthesized by ruthenium-catalyzed azide–alkyne cycloaddition (RuAAC), Scheme 1. The amide-linked compounds **17** and **18** were prepared by the reaction of acyl fluoride **35** with commercially available 4-aminobenzenesulfonamide or 3-aminobenzenesulfonamide, respectively, Scheme 2. Urea-linked CA inhibitors **19** and **20**

**Scheme 2. Synthesis of Amide-Linked Metallocene-Based CA Inhibitors 17 and 18<sup>a</sup>**



<sup>a</sup>Reagents and conditions: compound **35** (1.0 mmol) in DCM (5 mL), 3- or 4-aminobenzenesulfonamide (1.1 equiv) in DMF (0.35 mL) and pyridine (0.1 mL), rt, 5 days.

were synthesized indirectly from acyl fluoride **35** according to Scheme 3. Control compounds **21–26** were synthesized from azides **33** or **34** and commercially available phenyl acetylene (**21–24**) or TMS acetylene (**25–26**), similarly to Scheme 1. Note that removal of the TMS group using TBAF was required for the synthesis of **25**.

**Carbonic Anhydrase Inhibition Studies and Structure–Activity Relationships.** The enzyme inhibition data for **1–26** were obtained for the physiologically dominant CA I and II and tumor-associated transmembrane CA IX and XII, Table 1.

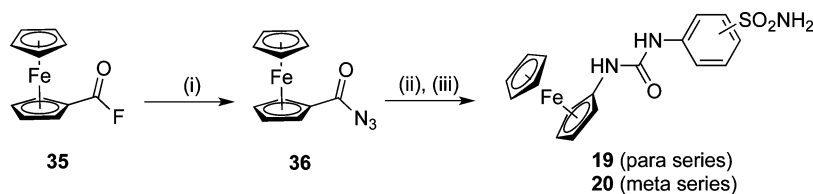
The regioisomeric compounds **25** and **26** provide a baseline to assess the impact of the metallocene substituent of triazoles

**1–4** and **5–8**, respectively, on CA inhibition. These controls comprise a 1,2,3-triazole that is linked either para (**25**) or meta (**26**) to the primary sulfonamide moiety of the benzenesulfonamide CA pharmacophore. Compound **25** is a weak inhibitor of CA I, II, and IX ( $K_i$ s 345–596 nM) and a moderate inhibitor of CA XII ( $K_i$  63 nM), while the meta regioisomer **26** has similarly weak inhibition at CA I ( $K_i$  = 618 nM) but moderate inhibition at CA II, IX, and XII ( $K_i$ s 41–68 nM). These inhibition data suggest that meta substitution relative to the primary sulfonamide functional group of the benzenesulfonamide CA anchor when compared to an identical para substituent has minimal effect on inhibition of CA I and XII, however, a greater impact is observed with isozymes II and IX, where meta substitution provided an order of magnitude improvement in CA inhibition. Control compounds **21–24** are related to compounds **25** and **26** but differ in comprising a phenyl–triazole tail fragment in place of the unsubstituted triazole tail fragment. Compounds **21–24** comprise both 4- and 5-phenyl substituted 1,2,3-triazoles and provide complex and informative SAR. The phenyl moiety is a flat and relatively compact aromatic system in contrast to the barrel-shaped sandwich structure of classical metallocenes. The meta- versus para-substitution had less impact in these control compounds than for the unsubstituted triazoles **25** and **26**. Compounds **23** and **24**, where the phenyl substituent is at the 5-position of the 1,2,3-triazole, were weak inhibitors of CA I ( $K_i$ s 509–542 nM), similarly to the unsubstituted triazoles **25** and **26**. The phenyl substituent in the para series compounds **21** and **23** improved CA inhibition by an order of magnitude over unsubstituted **25** at CA II, CA IX, and CA I (**21** only) with moderate inhibition at CA XII similarly to **25**. The phenyl substituent in the meta series compounds **22** and **24** exhibited a trend closely aligned to unsubstituted triazole **26** with one exception; compound **22** (the 4-phenyl substituted 1,2,3-triazole) was a ~10-fold more potent CA XII inhibitor ( $K_i$  = 5.8 nM) than **26**.

The 20 metallocene-based CA inhibitors, compounds **1–20**, comprise significant structural diversity. SAR is assessed in the context of SAR described above for control compounds **21–26** as well across a number of different structural groupings:

*i. Ferrocene-Triazole and Ruthenocene-Triazole Tails.* Compounds **1–8** comprise a metallocene–triazole tail moiety directly attached to the benzene sulfonamide pharmacophore and so are direct analogues of control compounds **21–26** described above. These inhibitors were synthesized by either CuAAC (**1**, **3**, **5**, and **7**) or RuAAC (**2**, **4**, **6**, and **8**) and so are 1,4- and 1,5-disubstituted triazoles, respectively. The metallocene substituent generally contributed to improved CA inhibition compared to the unsubstituted triazoles **25** and **26**. At CA I, the metallocene moiety exhibited similar SAR to the phenyl moiety (**21–24**), however, at CA II, IX, and XII, the metallocene moiety predominantly acted to improve CA

**Scheme 3. Synthesis of Urea-Linked Metallocene-Based CA Inhibitors 19 and 20<sup>a</sup>**



<sup>a</sup>Reagents and conditions: (i) compound **35** (4.3 mmol) in THF (2 mL), sodium azide (4.5 equiv) in water (10 mL), rt, 3 h; (ii) compound **36** (0.5 mmol), toluene, 100 °C, 1 h; then (iii) *p*- or *m*-aminobenzenesulfonamide (1.1 equiv), DMF (1 mL), 50 °C, 18 h.

Table 1. CA Inhibition Data for Compounds 1–26 against Human CA Isozymes I, II, IX, and XII

| compd (para series) | $K_i$ (nM) <sup>a</sup> |                    |                    |                     | compd (meta series) | $K_i$ (nM) <sup>a</sup> |                    |                    |                     |
|---------------------|-------------------------|--------------------|--------------------|---------------------|---------------------|-------------------------|--------------------|--------------------|---------------------|
|                     | CA I <sup>b</sup>       | CA II <sup>b</sup> | CA IX <sup>c</sup> | CA XII <sup>c</sup> |                     | CA I <sup>b</sup>       | CA II <sup>b</sup> | CA IX <sup>c</sup> | CA XII <sup>c</sup> |
| 1 <sup>d</sup>      | 3900                    | 80                 | 85                 |                     | 5                   | 1790                    | 4165               | 33.1               | 18.8                |
| 2 <sup>d</sup>      | 1600                    | 36                 | 65                 |                     | 6                   | 361                     | 3.2                | 5.9                | 6.8                 |
| 3 <sup>d</sup>      | 44                      | 9.7                | 10.3               |                     | 7                   | 70                      | 6.9                | 8.2                | 5.5                 |
| 4 <sup>d</sup>      | 9                       | 12.3               | 64                 |                     | 8                   | 54                      | 5.2                | 8.8                | 6.9                 |
| 9                   | 77                      | 7.1                | 80                 | 9.2                 | 12                  | 42                      | 3.8                | 9.6                | 7.9                 |
| 10                  | 76                      | 7.5                | 81                 | 8.0                 | 13                  | 43                      | 4.0                | 9.1                | 7.3                 |
| 11                  | 44                      | 4                  | 7.9                | 6.8                 | 14                  | 56                      | 5.2                | 8.1                | 7.0                 |
| 15                  | 2580                    | 415                | 75.5               | 8.7                 | 16                  | 3680                    | 4690               | 136                | 26.2                |
| 17                  | 101                     | 10.3               | 76.2               | 9.1                 | 18                  | 1890                    | 3720               | 186                | 31.5                |
| 19                  | 2180                    | 2570               | 137                | 21.1                | 20                  | 2290                    | 90.5               | 82.3               | 21.4                |
| 21                  | 60                      | 47                 | 72                 | 39                  | 22                  | 51                      | 45                 | 69                 | 5.8                 |
| 23                  | 542                     | 41                 | 61                 | 57                  | 24                  | 509                     | 46                 | 68                 | 42                  |
| 25                  | 433                     | 345                | 596                | 63                  | 26                  | 618                     | 52                 | 58                 | 46                  |

<sup>a</sup>Errors in the range of  $\pm 5$ –10% of the reported value, from three determinations. <sup>b</sup>Human (cloned) isozymes. <sup>c</sup>Catalytic domain of human (cloned) isozymes. <sup>d</sup>Previously reported in reference 7a.

inhibition compared to a phenyl moiety, with  $K_i$ s for compounds 3 and 6–8 each 10 nM or less at these isozymes. Of the para substituted compounds 1–4, the ruthenocene analogues 3 and 4 were better CA inhibitors across all CA isozymes than the ferrocene inhibitors 1 and 2, while of the meta substituted compounds 5–8, the ruthenocene analogues 7 and 8 were similar in potency to ferrocene-based inhibitor 6 yet better across all CA isozymes compared to ferrocene-based inhibitor 5. A notable difference in regioisomers activity was evident with the ferrocene analogues 5 and 6, with compound 6 significantly more potent than its regioisomer compound 5. Compound 6, the most potent ferrocene-based inhibitor, had  $K_i$ s ranging from 3.2 to 6.8 nM at CA II, IX, and XII. Differences in potency across the four ruthenocene analogues was less pronounced, for example, the ruthenocanyl 1,4- and 1,5-disubstituted triazole regioisomers (compounds 7 and 8) were of similar potency. The SAR we report surrounding the ferrocenyl and ruthenocanyl–triazole tails for the different CA isozymes is consistent with our SAR findings for recently reported regioisomeric CA inhibitors with carbohydrate–triazole tails prepared by both RuAAC<sup>16a</sup> and CuAAC.<sup>16c</sup> Here the barrel-shaped metallocene moiety has provided a way to discriminate the CA isozymes active site when compared to the corresponding phenyl analogues, further suggestive of a potentially valuable structural role for the organometallic fragment in continued CA inhibitor development for desired biological activity.

*ii. Covalent Linker to Tail Fragment.* A standout SAR from inspection of  $K_i$  values presented in Table 1 is the weaker CA inhibition observed for compounds 15–20 compared to other metallocene inhibitors of this study. Compounds 15–20 comprise an amide or urea covalent linker between the [aromatic]–[ZBG] CA pharmacophore and metallocene tail fragment, and while generally weaker as CA inhibitors, inhibition of cancer-associated isozymes IX and XII is greater than for off-target isozymes I and II, a sought after selectivity profile with CA inhibitor development. Esters 9 and 12 are biososteres of amides 15 and 16, yet the esters remarkably exhibit 2 orders of magnitude better CA I and II inhibition than their corresponding amides. The para-substituted compound 9 (ester) and 15 (amide) have similar potency at CA IX and XII, while the meta-substituted compound 12 (ester) was a better CA IX and XII inhibitor than its amide counterpart 16.

Increasing the length of the alkyl chain of the ester linkage (compare 9–11 and 12–14) had minimal effect on CA inhibition, with the exception of the longer chain compound 11, which was a 10-fold better CA IX inhibitor ( $K_i = 7.9$  nM) than the shorter chain ester 9 and 10.

*iii. para-Substitution and meta-Substitution.* The 10 para-substituted analogues (1–4, 9–11, 15, 17, 19) had CA I inhibition constants that ranged from 9 to 3900 nM, while the 10 meta-substituted analogues (5–8, 12–14, 16, 18, 20) had CA I inhibition constants that ranged from 42 to 3680 nM, both trends reflecting the impact of the considerable diversity present across the metallocene-based CA inhibitor library. Pairwise comparison of para- versus meta-substitution shows generally similar inhibition at CA I, while at CA II compounds are similar with a few notable compound pairs as exceptions (1 and 5, 2 and 6, 15 and 16, 17 and 18), all of which have the para-substitution pattern more potent than the meta-substitution pattern. At CA IX the meta-series compounds are generally good inhibitors and better than their corresponding para-series compounds. At CA XII many of the compounds, both para- and meta-, are very potent inhibitors with low nM inhibition constants. For the control compounds 21–24, the phenyl–triazole substituent displayed little difference between meta and para relationship across all isozymes (except for 21 versus 22 at CA XII).

**In Vitro ADME Properties.** The metallocene-based compounds in this study are good CA inhibitors in vitro, and in addition several compounds display selectivity for the cancer-associated CAs compared to off-target CAs. The design of useful drugs and/or probes for medicinal chemistry requires balancing compound activity with a number of different compound properties, with the knowledge that each impacts on the drugs performance in vivo. A recent analysis of compounds published in the medicinal chemistry literature demonstrated that there is a noticeable creep of compound properties outside recognized drug-like parameters,<sup>19</sup> and here we were keen to build an understanding of the impact of the ferrocene moiety on a selection of key drug-like parameters. We have experimentally measured and determined Log *P*, Log *D*, solubility, metabolism, and in vitro permeability for four CA inhibitors sharing the core structure of a disubstituted triazole benzenesulfonamide: two ferrocene-based compounds (regioisomers 1 and 5), and two analogues of 1, one where the

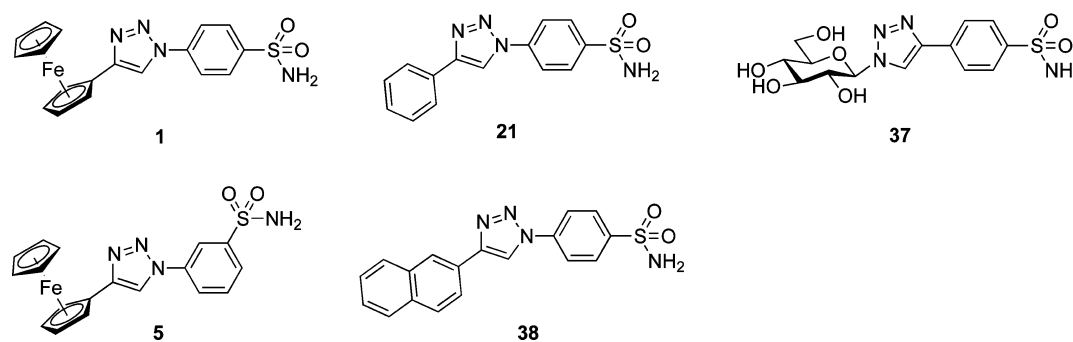


Figure 5. Compounds for ADME studies.

ferrocene is replaced by a phenyl moiety (compound **21**), and another where the ferrocene is replaced by a glucosyl moiety (compound **37**), Figure 5.<sup>16c</sup>

**Lipophilicity.** Log *P* and Log *D* describe a compound's lipophilicity, and values often correlate with a number of key biopharmaceutical parameters in drug discovery. Table 2 shows

Table 2. Partitioning Data for Test Compounds at 25 °C

| compd     | Log <i>D</i> <sub>7.4</sub> <sup>a</sup> | Log <i>D</i> <sub>3.0</sub> <sup>a</sup> | Log <i>D</i> <sub>7.4</sub> <sup>b</sup> | Log <i>D</i> <sub>3.0</sub> <sup>b</sup> | cLogP <sup>c</sup> |
|-----------|--|--|--|--|--------------------|
| <b>1</b>  | 2.9                                      | 2.9                                      | 2.9                                      | 2.1                                      |                    |
| <b>5</b>  | 2.9                                      | 2.9                                      | 3.0                                      | 2.7                                      |                    |
| <b>21</b> | 2.3                                      | 2.3                                      | 2.4                                      | 2.3                                      | 2.5                |
| <b>37</b> | -0.1                                     | -0.1                                     | <i>d</i>                                 | <i>d</i>                                 | -1.6               |
| <b>38</b> |  |  |  |  | 3.7                |

<sup>a</sup>Chromatographic estimation method. <sup>b</sup>Shake flask method. <sup>c</sup>Calculated using ChemDraw Ultra 12. <sup>d</sup>Concentration values were outside of the linear range of the assay.

experimental Log *P* and Log *D* values for compounds **1**, **5**, **21**, and **37** and calculated Log *P* (cLogP) values for compounds **21**, **37** and **38**. The Log *D* (Log *D* at pH 7.4 and pH 3.0) values were measured using both a RP-HPLC method<sup>20</sup> and the traditional shake flask method. As expected from the ionization properties of the compounds (expected to be neutral at both pH values), pH did not impact on the measured partition coefficients, Table 2. Ferrocene-based regioisomers **1** and **5** had similar Log *D*<sub>7.4</sub> and Log *D*<sub>3.0</sub> values, with values ~0.6 log units higher than for the phenyl compound **21**. This demonstrates that the ferrocene moiety is more strongly lipophilic than the phenyl moiety. As expected, carbohydrate-based compound (**37**) with four hydroxyl groups has a markedly reduced Log *D* value (Log *D*<sub>7.4</sub> or <sub>3.0</sub> of -0.1) compared to compounds **1**, **5**, and **21**, which is consistent with the increased hydrophilicity of **37**.

The use of software tools to predict Log *P* (cLogP) is now routine in medicinal chemistry, however, common programs lack a metallocene substructure in their training set. The experimentally measured octanol–water partition coefficient for ferrocene is 3.46.<sup>21</sup> This was of the same order as that measured for naphthalene (3.30) but much higher than that for benzene (2.13).<sup>21</sup> Using ChemDraw Ultra 12 software, the cLogP for the virtual compound **38**, where a naphthyl moiety replaces the ferrocenyl moiety of **1**, is 3.7. This value is 0.8 log units higher than the experimentally determined Log *D*<sub>7.4</sub> value for **1** and **5**. The cLogP for the phenyl compound **21** is 2.5 (close to the measured value) and is 0.4 log units lower than the experimentally determined Log *D*<sub>7.4</sub> value for **1** and **5**. The ferrocene moiety lipophilicity of compounds **1** and **5** is thus not well modeled by replacement with either a naphthyl or a phenyl

moiety as the measured Log *D* of ferrocene-based compounds **1** and **5** falls between the clogP values calculated for these two aromatics.

**Permeability.** The experimental lipophilicity results imply that compounds **1**, **5**, and **21** should exhibit good passive diffusion across gastrointestinal epithelial cells. The Caco-2 cell model was used to measure the in vitro permeability (*P*<sub>app</sub>) of compounds **1**, **5**, **21**, and **37**. Typical *P*<sub>app</sub> values for high permeability compounds are >2 × 10<sup>-5</sup> cm s<sup>-1</sup>, while for low permeability compounds are <2 × 10<sup>-6</sup> cm s<sup>-1</sup>. The experimental values of *P*<sub>app</sub> at pH 7.4 using the Caco-2 assay are presented in Table 3. For all compounds tested, there was

Table 3. Caco-2 Permeability Coefficients for Test Compounds

| compd       | <i>P</i> <sub>app</sub> (cm s <sup>-1</sup> ) <sup>a</sup> | std dev                | mass balance (%) |
|-------------|--|------------------------|------------------|
| <b>1</b>    | 5.8 × 10 <sup>-5</sup>                                     | 1.6 × 10 <sup>-5</sup> | 83               |
| <b>5</b>    | 6.1 × 10 <sup>-5</sup>                                     | 1.5 × 10 <sup>-5</sup> | 87               |
| <b>21</b>   | 5.8 × 10 <sup>-5</sup>                                     | 8.5 × 10 <sup>-6</sup> | 84               |
| <b>37</b>   | ND <sup>b</sup>  | ND <sup>b</sup>        | 90               |
| mannitol    | 1.7 × 10 <sup>-6</sup>                                     | 7.0 × 10 <sup>-7</sup> | 100              |
| propranolol | 4.2 × 10 <sup>-5</sup>                                     | 2.9 × 10 <sup>-6</sup> | 100              |

<sup>a</sup>Average of 3–4 determinations. <sup>b</sup>ND = not determined as compound **37** was not detected in the acceptor chamber. Mannitol and propranolol were included as low and high permeability markers, respectively.

good mass balance (>80%) indicating minimal retention of compounds within the cell monolayer and minimal nonspecific adsorption. *P*<sub>app</sub> values for the control compounds mannitol (low permeability marker) and propranolol (high permeability marker) were consistent with historical results. Compounds **1**, **5**, and **21** have *P*<sub>app</sub> values consistent with high permeability and good oral absorption. The *P*<sub>app</sub> values for **1**, **5**, and **21** are very similar, indicating that the ferrocene and phenyl moieties similarly contribute to membrane permeability in this model. For the carbohydrate-based compound (**37**), no compound was detected in the acceptor chamber (below the analytical lower limit of quantitation), indicative of a compound with very low permeability. The permeability results are in agreement with predictions based on experimental lipophilicity.

**Solubility.** Solubility is another property that can significantly affect oral absorption of a drug. The kinetic and equilibrium solubility results for the four test compounds (at pH 2.0, pH 6.5, and in water) are presented in Table 4. The kinetic solubility results (presented as a range) exhibited a similar trend to the equilibrium solubility results, although the absolute values differ. The glycoconjugate CA inhibitor **37** has

Table 4. Solubility Data for the Test Compounds at 25 °C

| compd | kinetic solubility (pH 2) <sup>a</sup> | equilibrium solubility (pH 2) <sup>b</sup> | kinetic solubility (pH 6.5) <sup>a</sup> | equilibrium solubility (pH 6.5) <sup>b</sup> | equilibrium solubility (water) <sup>b</sup> |
|-------|--|--|--|--|---|
| 1     | <1.6                                   | 5.0  | <1.6                                     | 1.7  | 0.7   |
| 5     | 6.3–12.5                               | 26.0                                       | 6.3–12.5                                 | 5.1  | 21.6  |
| 21    | 1.6–3.1                                | 1.5  | 1.6–3.1                                  | 1.4  | 2.2   |
| 37    | 25.0–50.0                              | 905  | 25.0–50.0                                | 978  | 1088  |

<sup>a</sup>Kinetic solubility results determined using the nephelometric screening method,  $\mu\text{g}/\text{mL}$ . <sup>b</sup>Equilibrium solubility results quoted represent 24 h data,  $\mu\text{g}/\text{mL}$ .

Table 5. Metabolic Stability Parameters for Test Compounds Based on NADPH-Dependent Degradation Profiles in Human Liver Microsomes

| compd | degradation half-life (min) <sup>a</sup> | in vitro $\text{CL}_{\text{int}}$ ( $\mu\text{L}/\text{min}/\text{mg}$ protein) <sup>a</sup> | microsome-predicted $\text{EH}^a$ | metabolites detected <sup>b</sup> |
|-------|--|--|-----------------------------------|-----------------------------------|
| 1     | 212 $\pm$ 57.0                           | 8.6 $\pm$ 2.3  | 0.32 $\pm$ 0.06                   | none                              |
| 5     | 123 $\pm$ 26.7                           | 15 $\pm$ 3.6   | 0.44 $\pm$ 0.06                   | none                              |
| 21    | 354 $\pm$ 822                            | 5.1 $\pm$ 1.1  | 0.22 $\pm$ 0.04                   | none                              |
| 37    | 279 $\pm$ 124                            | 7.4 $\pm$ 4.1  | 0.28 $\pm$ 0.11                   | none                              |

<sup>a</sup>Values are represented as mean  $\pm$  SD ( $n = 3$ ). <sup>b</sup>The metabolite search strategy was directed toward potential products of oxygenation, bis-oxygenation, oxygenation plus glucuronidation, and *N*-dealkylation.

moderate kinetic solubility and good equilibrium solubility, suggesting that the kinetic solubility assay underestimates the actual solubility of this compound. Metallocene compound **1** and phenyl compound **21** were found to be sparingly soluble under both kinetic and equilibrium conditions. Interestingly, metallocene compound **5**, the regioisomer of compound **1**, has moderate solubility, with values reasonably consistent under both kinetic and equilibrium conditions.

**Metabolic Stability.** Next we determined the *in vitro* metabolic stability of the four compounds using human liver microsomes as a preliminary indication of the likely *in vivo* metabolic clearance and to see if any metabolic products could be detected. The four test compounds exhibited low to moderate rates of degradation in human liver microsomes, and no metabolites were detected for any of the test compounds. On the basis of the *in vitro* intrinsic clearance values, these compounds would be expected to be subject to low to intermediate hepatic clearances *in vivo*. There was no apparent degradation of the compounds in microsomal matrix in the absence of cofactors, suggesting that the apparent rates of degradation in the presence of cofactor were due solely to cofactor-dependent microsomal metabolism. There was also no major increase in the rate of degradation observed in microsomal samples containing NADPH and UDPGA (supplemented with the pore-forming peptide, alamethicin) relative to NADPH alone, suggesting that these compounds were not susceptible to primary glucuronidation in the microsomal test system, Table 5.

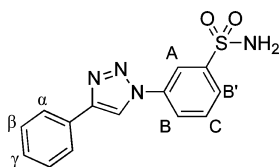
## CONCLUSIONS

In this study, 20 metallocene-based CA inhibitors (compounds **1**–**20**) comprising extensive structural diversity were synthesized and evaluated as CA inhibitors. These compounds were moderate to good CA inhibitors *in vitro*, and several compounds displayed selectivity for the cancer-associated CAs compared to off-target CAs. At CA I, the metallocene moiety exhibited similar SAR to the phenyl moiety (compounds **21**–**24**), however, at CA II, IX, and XII, the metallocene moiety predominantly acted to improve CA inhibition compared to a phenyl moiety. The SAR surrounding the ferrocenyl and ruthenocenyl–triazole tails for the different

CA isozymes is consistent with our SAR findings for recently reported regioisomeric CA inhibitors with carbohydrate–triazole tails prepared also by CuAAC or RuAAC. The measured *Log P*, *Log D*, solubility, metabolism, and *in vitro* permeability of two ferrocene-based compounds (regioisomers **1** and **5**) and the phenyl and glucosyl analogues of **1** (compounds **21** and **37**, respectively) resulted in values consistent with the general structural features of the compounds. Compounds, **1**, **5**, and **21** were found to have characteristics consistent with lipophilic compounds. Compound **37** is less lipophilic than the other three compounds; this was reflected in the solubility and partition coefficient values for this compound. A significant finding with implications for the study of metallocene-based compounds in medicinal chemistry is that the ferrocene moiety lipophilicity is not well modeled by replacement with either naphthyl or a phenyl standard aromatic rings. The measured *Log D* of ferrocene-based compounds **1** and **5** falls between the *clogP* values calculated for either the naphthyl or the phenyl analogue. The barrel-shaped metallocene moiety has provided a means to discriminate the CA isozymes active site when compared to the corresponding phenyl analogues, while biopharmaceutical properties were typically similar. These compounds may constitute potentially valuable leads for the development of CA inhibitor-based therapeutics and provide further support for the application of metallocenes in CA inhibitor development.

## EXPERIMENTAL SECTION

**Chemistry.** All starting materials were purchased from commercial suppliers. Known building blocks were either commercially available (**27**), synthesized as reported by us earlier (**28**,<sup>7a</sup> **33**<sup>16d</sup>), or synthesized according to literature (**35**<sup>17</sup>). All reactions were monitored by TLC using silica plates with visualization of product bands by UV fluorescence ( $\lambda = 254$  nm) and ninhydrin. Silica gel flash chromatography was performed using silica gel 60 Å (230–400 mesh). NMR (<sup>1</sup>H, <sup>13</sup>C {<sup>1</sup>H}), gCOSY, and HSQC) spectra were recorded on a 500 MHz spectrometer at 30 °C. Chemical shifts for <sup>1</sup>H and <sup>13</sup>C NMR acquired in DMSO-*d*<sub>6</sub> are reported in ppm relative to residual solvent proton ( $\delta = 2.50$  ppm) and carbon ( $\delta = 39.5$  ppm) signals, respectively. Chemical shifts for <sup>1</sup>H NMR acquired in CDCl<sub>3</sub> are reported in ppm relative to residual solvent proton ( $\delta = 7.26$  ppm). Multiplicity is indicated as follows: s (singlet); d (doublet); t (triplet);



m (multiplet); dd (doublet of doublet); ddd (doublet of doublet of doublet); br (broad). Coupling constants are reported in hertz (Hz). Labeling of compounds used for NMR assignments is shown below.

Melting points are uncorrected. High- and low-resolution mass spectra were acquired using electrospray as the ionization technique in positive ion and/or negative ion modes as stated. All MS analysis samples were prepared as solutions in methanol. All compounds were analyzed for purity by HPLC with both UV (200–400 nm) and evaporative light scattering detection (ELSD) detection used. Purity of all compounds was  $\geq 95\%$ .

**General Procedure 1. Synthesis of 1,4-Disubstituted-1,2,3-triazoles by CuAAC.** A mixture of azide (0.02–0.1 M) and alkyne (1.0 equiv) in *tert*-butyl alcohol and water (1:1) with  $\text{CuSO}_4 \cdot 5\text{H}_2\text{O}$  (0.2 equiv) and sodium ascorbate (0.4 equiv) was stirred vigorously overnight (18 h) at 40 °C under a nitrogen atmosphere. The precipitate that formed was collected by vacuum filtration, washed with water, and purified by flash chromatography (1:1 ethyl acetate:*n*-hexane, then 100% ethyl acetate) using solid addition from ethyl acetate.

**General Procedure 2. Synthesis of 1,5-Disubstituted-1,2,3-triazoles by RuAAC.** A mixture of azide (0.02–0.15 M) and alkyne (1.0 equiv) in toluene with  $[\text{Cp}^*\text{RuCl}(\text{PPh}_3)_2]$  or  $[\text{Cp}^*\text{RuCl}(\text{cod})]$  (5 mol %) was heated (100 °C) with stirring overnight (18 h). The reaction solvent was removed in vacuo and the remaining residue purified by flash chromatography (1:1 ethyl acetate:*n*-hexane, then 100% ethyl acetate).

**General Procedure 3. Synthesis of alkyne building blocks 29–32.** A mixture of fluorocarbonylferrocene **35** (1.0 mmol), corresponding alcohol or amine (1.0–1.5 equiv), and 4-dimethylaminopyridine (1.0–1.5 equiv) were prepared in DCM and stirred at rt for 20 h. The reaction solvent was removed in vacuo, and the remaining residue dissolved in ethyl acetate, washed with brine (2  $\times$  30 mL), dried ( $\text{MgSO}_4$ ), and solvent removed. Compounds were used as substrates in general procedure 1 without further purification.

**3-(4-Ferrocenyl-1H-1,2,3-triazol-1-yl)benzenesulfonamide (5).** The title compound was prepared from fragments **27** and **34** according to general procedure 1 and isolated as an orange solid (154 mg, 0.38 mmol, 75%); mp 186–188 °C.  $^1\text{H}$  NMR (500 MHz,  $\text{DMSO}-d_6$ ):  $\delta$  9.02 (s, 1H, triazole CH), 8.41 (s, 1H,  $\text{Ar}-\text{H}_A$ ), 8.16–8.17 (m, 1H,  $\text{Ar}-\text{H}_{B \text{ or } B'}$ ), 7.92–7.94 (m, 1H,  $\text{Ar}-\text{H}_{B \text{ or } B'}$ ), 7.82–7.85 (m, 1H,  $\text{Ar}-\text{H}_C$ ), 7.58 (s, 2H,  $\text{SO}_2\text{NH}_2$ ), 4.81–4.82 (m, 2H, Cp-H), 4.36–4.38 (m, 2H, Cp-H), 4.09 (s, 5H, unsubstituted Cp-H).  $^{13}\text{C}$   $\{^1\text{H}\}$  NMR (125 MHz,  $\text{DMSO}-d_6$ ):  $\delta$  147.0 (triazole C or *Ar*-C), 145.7 (*Ar*-C or triazole C), 136.7 (*Ar*-C), 130.8 (*Ar*- $\text{CH}_A$ ), 125.2 (*Ar*- $\text{CH}_{B \text{ or } B'}$ ), 122.7 (*Ar*- $\text{CH}_{B \text{ or } B'}$ ), 118.5 (triazole CH), 116.8 (*Ar*- $\text{CH}_C$ ), 74.9 (Cp-C), 69.3 (unsubstituted Cp), 68.6 (Cp-CH), 66.5 (Cp-CH). LRMS ( $\text{ESI}^+$ ):  $m/z$  407.3  $[\text{M} + \text{H}]^+$ . HRMS ( $\text{ESI}$ ) calcd for  $\text{C}_{18}\text{H}_{16}\text{FeN}_4\text{O}_2\text{SH}$  407.0463, found 407.0450.

**3-(5-Ferrocenyl-1H-1,2,3-triazol-1-yl)benzenesulfonamide (6).** The title compound was prepared from fragments **27** and **34** according to general procedure 2 and isolated as an orange solid (86 mg, 0.21 mmol, 42%); mp 184–186 °C.  $^1\text{H}$  NMR (500 MHz,  $\text{DMSO}-d_6$ ):  $\delta$  8.11 (s, 1H, triazole CH), 8.07–8.08 (m, 1H,  $\text{Ar}-\text{H}_{B \text{ or } B'}$ ), 7.98 (s, 1H,  $\text{Ar}-\text{H}_A$ ), 7.82–7.85 (m, 1H,  $\text{Ar}-\text{H}_C$ ), 7.75–7.76 (m, 1H,  $\text{Ar}-\text{H}_{B \text{ or } B'}$ ), 7.60 (br s, 2H,  $\text{SO}_2\text{NH}_2$ ), 4.35–4.36 (m, 2H, Cp-H), 4.26 (s, 2H, Cp-H), 4.12 (s, 5H, unsubstituted Cp-H).  $^{13}\text{C}$   $\{^1\text{H}\}$  NMR (125 MHz,  $\text{DMSO}-d_6$ ):  $\delta$  145.4 (*Ar*-C), 137.5 (triazole C), 136.8 (*Ar*-C), 132.1 (triazole CH), 130.4 (*Ar*- $\text{CH}_C$ ), 129.7 (*Ar*- $\text{CH}_{B \text{ or } B'}$ ), 127.0 (*Ar*- $\text{CH}_{B \text{ or } B'}$ ), 123.8 (*Ar*- $\text{CH}_A$ ), 69.6 (unsubstituted Cp-CH), 69.4 (Cp-CH), 67.8 (Cp-CH), Cp-C not detected. LRMS ( $\text{ESI}^+$ ):  $m/z$  407.3  $[\text{M}$

+  $\text{H}]^+$ . HRMS ( $\text{ESI}$ ) calcd for  $\text{C}_{18}\text{H}_{16}\text{FeN}_4\text{O}_2\text{SH}$  407.0463, found 407.0447.

**3-(4-Ruthenocenyl-1H-1,2,3-triazol-1-yl)benzenesulfonamide (7).** The title compound was prepared from fragments **28** and **34** according to general procedure 1 and isolated as an off-white solid (10 mg, 0.02 mmol, 22%); mp 211–212 °C.  $^1\text{H}$  NMR (500 MHz,  $\text{DMSO}-d_6$ ):  $\delta$  8.89 (s, 1H, triazole CH), 8.36 (s, 1H,  $\text{Ar}-\text{H}_A$ ), 8.11–8.12 (m, 1H,  $\text{Ar}-\text{H}_{B \text{ or } B'}$ ), 7.90–7.92 (m, 1H,  $\text{Ar}-\text{H}_{B \text{ or } B'}$ ), 7.80–7.83 (m, 1H,  $\text{Ar}-\text{H}_C$ ), 7.57 (s, 2H,  $\text{SO}_2\text{NH}_2$ ), 5.22 (s, 2H, Cp-H), 4.73 (s, 2H, Cp-H), 4.53 (s, 5H, unsubstituted Cp-H).  $^{13}\text{C}$   $\{^1\text{H}\}$  NMR (125 MHz,  $\text{DMSO}-d_6$ ):  $\delta$  146.3 (triazole C or *Ar*-C), 145.7 (*Ar*-C or triazole C), 136.7 (*Ar*-C), 130.8 (*Ar*- $\text{CH}_A$ ), 125.2 (*Ar*- $\text{CH}_{B \text{ or } B'}$ ), 122.7 (*Ar*- $\text{CH}_{B \text{ or } B'}$ ), 118.7 (triazole CH), 116.8 (*Ar*- $\text{CH}_C$ ), 78.6 (Cp-C), 71.3 (unsubstituted Cp), 71.0 (Cp-CH), 69.2 (Cp-CH). LRMS ( $\text{ESI}^-$ ):  $m/z$  447.2  $[\text{M} - \text{H}]^-$ . HRMS ( $\text{ESI}$ ) calcd for  $\text{C}_{18}\text{H}_{16}\text{RuN}_4\text{O}_2\text{SH}$  449.0143, found 449.0123.

**3-(5-Ruthenocenyl-1H-1,2,3-triazol-1-yl)benzenesulfonamide (8).** The title compound was prepared from fragments **28** and **34** according to general procedure 2 and isolated as an off-white solid (58 mg, 0.13 mmol, 26%); mp 184–186 °C (decomp).  $^1\text{H}$  NMR (600 MHz,  $\text{DMSO}-d_6$ ):  $\delta$  9.41 (s, 1H, triazole CH), 8.49 (s, 1H,  $\text{Ar}-\text{H}_A$ ), 8.24–8.26 (m, 1H,  $\text{Ar}-\text{H}_{B \text{ or } B'}$ ), 7.95–7.97 (m, 1H,  $\text{Ar}-\text{H}_{B \text{ or } B'}$ ), 7.83–7.85 (m, 1H,  $\text{Ar}-\text{H}_C$ ), 7.59 (s, 2H,  $\text{SO}_2\text{NH}_2$ ), 5.66 (s, 2H, Cp-H), 5.01 (s, 2H, Cp-H), 4.60 (s, 5H, unsubstituted Cp-H).  $^{13}\text{C}$   $\{^1\text{H}\}$  NMR (150 MHz,  $\text{DMSO}-d_6$ ):  $\delta$  147.8 (triazole C), 145.7 (*Ar*-C), 136.3 (*Ar*-C), 130.8 (*Ar*- $\text{CH}_C$ ), 126.1 (triazole CH), 125.9 (*Ar*- $\text{CH}_{B \text{ or } B'}$ ), 123.6 (*Ar*- $\text{CH}_{B \text{ or } B'}$ ), 117.8 (*Ar*- $\text{CH}_A$ ), 82.5 (Cp-C), 74.1 (Cp-CH), 72.3 (Cp-CH), 72.2 (unsubstituted Cp-CH). LRMS ( $\text{ESI}^-$ ):  $m/z$  447.3  $[\text{M} - \text{H}]^-$ . HRMS ( $\text{ESI}$ ) calcd for  $\text{C}_{18}\text{H}_{16}\text{RuN}_4\text{O}_2\text{SH}$  449.0143, found 449.0131.

**(1-(4-Sulfamoylphenyl)-1H-1,2,3-triazol-4-yl)methyl Ferrocenyl-1-carboxylate (9).** The title compound was prepared from fragments **29** and **33** according to general procedure 1 and isolated as an orange solid (51 mg, 0.11 mmol, 44%); mp 254–255 °C (decomposed).  $^1\text{H}$  NMR (500 MHz,  $\text{DMSO}-d_6$ ):  $\delta$  9.04 (s, 1H, triazole CH), 8.16–8.17 (m, 2H, *Ar*-H), 8.01–8.03 (m, 2H, *Ar*-H), 7.50 (s, 2H,  $\text{SO}_2\text{NH}_2$ ), 5.40 (s, 2H,  $\text{CH}_2$ ), 4.79 (s, 2H, Cp-H), 4.50 (s, 2H, Cp-H), 4.17 (s, 5H, unsubstituted Cp-H).  $^{13}\text{C}$   $\{^1\text{H}\}$  NMR (125 MHz,  $\text{DMSO}-d_6$ ):  $\delta$  171.1 (C=O), 144.6 (triazole C and *Ar*-C), 139.2 (*Ar*-C), 128.2 (*Ar*-CH), 123.8 (triazole CH), 121.1 (*Ar*-CH), 72.3 (Cp-CH), 70.9 (Cp-C), 70.6 (Cp-CH), 70.3 (unsubstituted Cp-CH), 57.4 ( $\text{CH}_2$ ). LRMS ( $\text{ESI}^+$ ):  $m/z$  489.0  $[\text{M} + \text{Na}]^+$ . HRMS ( $\text{ESI}$ ) calcd for  $\text{C}_{20}\text{H}_{18}\text{FeN}_4\text{O}_4\text{SNa}$  487.0034, found 487.0314.

**2-(1-(4-Sulfamoylphenyl)-1H-1,2,3-triazol-4-yl)ethyl Ferrocenyl-1-carboxylate (10).** The title compound was prepared from fragments **30** and **33** according to general procedure 1 and isolated as an orange solid (108 mg, 0.22 mmol, 90%); mp 216–217 °C.  $^1\text{H}$  NMR (500 MHz,  $\text{DMSO}-d_6$ ):  $\delta$  8.86 (s, 1H, triazole CH), 8.11–8.13 (m, 2H, *Ar*-H), 8.00–8.02 (m, 2H, *Ar*-H), 7.48 (s, 2H,  $\text{SO}_2\text{NH}_2$ ), 4.73 (s, 2H, Cp-H), 4.49 (t,  $^3J_{\text{CH}-\text{CH}} = 5$  Hz, 2H,  $\alpha\text{-CH}_2$ ), 4.46 (s, 2H, Cp-H), 3.18 (t,  $^3J_{\text{CH}-\text{CH}} = 5$  Hz, 2H,  $\beta\text{-CH}_2$ ).  $^{13}\text{C}$   $\{^1\text{H}\}$  NMR (100 MHz,  $\text{DMSO}-d_6$ ):  $\delta$  170.5 (C=O), 145.1 (triazole C), 143.6 (*Ar*-C), 138.6 (*Ar*-C), 127.5 (*Ar*-CH), 121.1 (triazole CH), 119.9 (*Ar*-CH), 71.3 (Cp-CH), 70.5 (Cp-C), 69.7 (Cp-CH), 69.4 (unsubstituted Cp-CH), 62.4 ( $\alpha\text{-CH}_2$ ), 25.0 ( $\beta\text{-CH}_2$ ). LRMS ( $\text{ESI}^+$ ):  $m/z$  480.0  $[\text{M} + \text{H}]^+$ . HRMS ( $\text{ESI}$ ) calcd for  $\text{C}_{21}\text{H}_{20}\text{FeN}_4\text{O}_4\text{SNa}$  501.0494, found 501.0480.

**3-(1-(4-Sulfamoylphenyl)-1H-1,2,3-triazol-4-yl)propyl Ferrocenyl-1-carboxylate (11).** The title compound was prepared from fragments **31** and **33** according to general procedure 1 and isolated as an orange solid (119 mg, 0.24 mmol, 96%); mp 175–176 °C.  $^1\text{H}$  NMR (500 MHz,  $\text{DMSO}-d_6$ ):  $\delta$  8.76 (s, 1H, triazole CH), 8.10–8.12 (m, 2H, *Ar*-CH), 8.00–8.02 (m, 2H, *Ar*-CH), 7.49 (s, 2H,  $\text{SO}_2\text{NH}_2$ ), 4.75 (s, 2H, Cp-CH), 4.48 (s, 2H, Cp-CH), 4.27 (t,  $^3J_{\text{CH}-\text{CH}} = 7.5$  Hz, 2H,  $\alpha\text{-CH}_2$ ), 4.24 (s, 5H, unsubstituted Cp-CH), 2.91 (t,  $^3J_{\text{CH}-\text{CH}} = 7.5$  Hz, 2H,  $\gamma\text{-CH}_2$ ), 2.11 (dt,  $^3J_{\text{CH}-\text{CH}} = 7.5$  Hz,  $^3J_{\text{CH}-\text{CH}} = 7.5$  Hz, 2H,  $\beta\text{-CH}_2$ ).  $^{13}\text{C}$   $\{^1\text{H}\}$  NMR (125 MHz,  $\text{DMSO}-d_6$ ):  $\delta$  170.5 (C=O), 147.7 (triazole C), 143.5 (*Ar*-C), 138.7 (*Ar*-C), 127.4 (*Ar*-CH), 120.5 (triazole CH), 119.9 (*Ar*-CH), 71.3 (Cp-CH), 70.8 (Cp-C), 69.6 (Cp-CH), 69.5 (unsubstituted Cp-CH), 62.9 ( $\alpha\text{-CH}_2$ ), 27.9 ( $\beta\text{-CH}_2$ ), 21.6



( $\gamma$ -CH<sub>2</sub>). LRMS (ESI<sup>-</sup>):  $m/z$  493.2 [M - H]<sup>-</sup>. HRMS (ESI) calcd for C<sub>22</sub>H<sub>22</sub>FeN<sub>4</sub>O<sub>4</sub>Na 515.0650, found 515.0662.

**(1-(3-Sulfamoylphenyl)-1H-1,2,3-triazol-4-yl)methyl Ferrocenyl-1-carboxylate (12).** The title compound was prepared from fragments 29 and 34 according to general procedure 1 and isolated as an orange solid (63 mg, 0.14 mmol, 54%); mp 200–201 °C. <sup>1</sup>H NMR (500 MHz, DMSO-*d*<sub>6</sub>):  $\delta$  9.03 (s, 1H, triazole CH), 8.40 (s, 1H, Ar-H<sub>A</sub>), 8.15–8.17 (m, 1H, Ar-H<sub>B</sub> or B'), 7.91–7.93 (m, 1H, Ar-H<sub>B'</sub> or B), 7.80–7.83 (m, 1H, Ar-H<sub>C</sub>), 7.56 (br s, 2H, SO<sub>2</sub>NH<sub>2</sub>), 5.40 (s, 2H, CH<sub>2</sub>), 4.79 (s, 2H, Cp-H), 4.50 (s, 2H, Cp-H), 4.16 (s, 5H, unsubstituted Cp-H). <sup>13</sup>C {<sup>1</sup>H} NMR (125 MHz, DMSO-*d*<sub>6</sub>):  $\delta$  170.3 (C=O), 145.7 (triazole C), 143.8 (Ar-C), 136.5 (Ar-C), 130.9 (Ar-CH<sub>C</sub>), 125.5 (Ar-CH<sub>B'</sub> or B), 123.1 (Ar-CH<sub>B</sub> or B'), 123.1 (triazole CH), 117.2 (Ar-CH<sub>A</sub>), 71.5 (Cp-CH), 70.1 (Cp-C), 69.8 (Cp-CH), 69.5 (unsubstituted Cp-CH), 56.6 (CH<sub>2</sub>). LRMS (ESI<sup>-</sup>):  $m/z$  465.2 [M - H]<sup>-</sup>.

**2-(1-(3-Sulfamoylphenyl)-1H-1,2,3-triazol-4-yl)ethyl Ferrocenyl-1-carboxylate (13).** The title compound was prepared from fragments 30 and 34 according to general procedure 1 and isolated as an orange solid (100 mg, 0.21 mmol, 84%); mp 167–168 °C. <sup>1</sup>H NMR (500 MHz, DMSO-*d*<sub>6</sub>):  $\delta$  8.86 (s, 1H, triazole CH), 8.38 (s, 1H, Ar-H<sub>A</sub>), 8.11–8.12 (m, 1H, Ar-H<sub>B</sub> or B'), 7.89–7.90 (m, 1H, Ar-H<sub>B'</sub> or B), 7.80–7.82 (m, 1H, Ar-H<sub>C</sub>), 7.56 (s, 2H, SO<sub>2</sub>NH<sub>2</sub>), 4.73 (s, 2H, Cp-H), 4.50 (t, <sup>3</sup>J<sub>CH-CH</sub> = 7.5 Hz, 2H,  $\alpha$ -CH<sub>2</sub>), 4.46 (s, 2H, Cp-H), 4.10 (s, 5H, unsubstituted Cp-H), 3.18 (t, <sup>3</sup>J<sub>CH-CH</sub> = 7.5 Hz, 2H,  $\beta$ -CH<sub>2</sub>). <sup>13</sup>C {<sup>1</sup>H} NMR (125 MHz, DMSO-*d*<sub>6</sub>):  $\delta$  170.5 (C=O), 147.8 (triazole C), 145.1 (Ar-C), 136.8 (Ar-C), 130.9 (Ar-CH<sub>C</sub>), 125.3 (Ar-CH<sub>B</sub> or B'), 122.7 (Ar-CH<sub>B'</sub> or B), 121.2 (triazole CH), 116.9 (Ar-CH<sub>A</sub>), 71.3 (Cp-CH), 70.6 (Cp-C), 69.7 (Cp-CH), 69.4 (unsubstituted Cp-CH), 62.5 ( $\alpha$ -CH<sub>2</sub>), 25.1 ( $\beta$ -CH<sub>2</sub>). LRMS (ESI<sup>-</sup>):  $m/z$  479.3 [M - H]<sup>-</sup>.

**3-(1-(3-Sulfamoylphenyl)-1H-1,2,3-triazol-4-yl)propyl Ferrocenyl-1-carboxylate (14).** The title compound was prepared from fragments 31 and 34 according to general procedure 1 and isolated as an orange solid (111 mg, 0.22 mmol, 90%); mp 159–161 °C. <sup>1</sup>H NMR (500 MHz, DMSO-*d*<sub>6</sub>):  $\delta$  8.76 (s, 1H, triazole CH), 8.37 (s, 1H, Ar-H<sub>A</sub>), 8.09–8.11 (m, 1H, Ar-H<sub>B</sub> or B'), 7.89–7.91 (m, 1H, Ar-H<sub>B'</sub> or B), 7.78–7.82 (m, 1H, Ar-H<sub>C</sub>), 7.55 (s, 2H, SO<sub>2</sub>NH<sub>2</sub>), 4.75 (s, 2H, Cp-H), 4.48 (s, 2H, Cp-H), 4.26 (t, <sup>3</sup>J<sub>CH-CH</sub> = 7.5 Hz, 2H,  $\alpha$ -CH<sub>2</sub>), 4.23 (s, 5H, unsubstituted Cp-H), 2.91 (t, <sup>3</sup>J<sub>CH-CH</sub> = 7.5 Hz,  $\gamma$ -CH<sub>2</sub>), 2.11 (dt, <sup>3</sup>J<sub>CH-CH</sub> = 7.5 Hz, <sup>3</sup>J<sub>CH-CH</sub> = 7.5 Hz, 2H,  $\beta$ -CH<sub>2</sub>). <sup>13</sup>C {<sup>1</sup>H} NMR (125 MHz, DMSO-*d*<sub>6</sub>):  $\delta$  170.6 (C=O), 147.7 (triazole C), 145.7 (Ar-C), 136.8 (Ar-C), 130.8 (Ar-CH<sub>C</sub>), 125.1 (Ar-CH<sub>B</sub> or B'), 122.7 (Ar-CH<sub>B'</sub> or B), 120.5 (triazole CH), 116.9 (Ar-CH<sub>A</sub>), 71.3 (Cp-CH), 70.8 (Cp-C), 69.7 (Cp-CH), 69.5 (unsubstituted Cp-CH), 63.0 ( $\alpha$ -CH<sub>2</sub>), 27.9 ( $\beta$ -CH<sub>2</sub>), 21.7 ( $\gamma$ -CH<sub>2</sub>). LRMS (ESI<sup>-</sup>):  $m/z$  493.2 [M - H]<sup>-</sup>.

**N-(1-(4-Sulfamoylphenyl)-1H-1,2,3-triazol-4-yl)methyl Ferrocenyl-1-carboxamide (15).** The title compound was prepared from fragments 32 and 33 according to general procedure 1 and isolated as an orange solid (93 mg, 0.20 mmol, 80%); mp 181–183 °C. <sup>1</sup>H NMR (500 MHz, DMSO-*d*<sub>6</sub>):  $\delta$  8.76 (s, 1H, triazole CH), 8.40 (br s, 1H, NH), 8.14–8.16 (m, 2H, Ar-H), 8.00–8.02 (m, 2H, Ar-H), 7.50 (s, 2H, SO<sub>2</sub>NH<sub>2</sub>), 4.84 (s, 2H, Cp-H), 4.55 (d, <sup>3</sup>J<sub>CH-NH</sub> = 6 Hz, 2H, CH<sub>2</sub>), 4.36 (s, 2H, Cp-H), 4.14 (s, 5H, unsubstituted Cp-H). <sup>13</sup>C {<sup>1</sup>H} NMR (125 MHz, DMSO-*d*<sub>6</sub>):  $\delta$  169.8 (C=O), 147.6 (triazole C), 144.4 (Ar-C), 139.4 (Ar-C), 128.2 (Ar-CH), 122.0 (triazole CH), 120.8 (Ar-CH), 76.9 (Cp-C), 70.7 (Cp-CH), 70.0 (unsubstituted Cp-CH), 69.0 (Cp-CH), 35.0 (CH<sub>2</sub>). LRMS (ESI<sup>-</sup>):  $m/z$  464.3 [M - H]<sup>-</sup>.

**N-(1-(3-Sulfamoylphenyl)-1H-1,2,3-triazol-4-yl)methyl Ferrocenyl-1-carboxamide (16).** The title compound was prepared from fragments 32 and 34 according to general procedure 1 and isolated as an orange solid (90 mg, 0.19 mmol, 19%); mp 175–177 °C. <sup>1</sup>H NMR (500 MHz, DMSO-*d*<sub>6</sub>):  $\delta$  8.73 (s, 1H, triazole CH), 8.38–8.39 (m, 2H, Ar-H<sub>A</sub> and NH), 8.13–8.14 (m, 1H, Ar-H<sub>B</sub> or B'), 7.89–7.90 (m, 1H, Ar-H<sub>B'</sub> or B), 7.78–7.81 (m, 1H, Ar-H<sub>C</sub>), 7.55 (s, 2H, SO<sub>2</sub>NH<sub>2</sub>), 4.83 (s, 2H, Cp-H), 4.54 (d, <sup>3</sup>J<sub>CH-NH</sub> = 5 Hz), 4.35 (s, 2H, Cp-H), 4.13 (s, 5H, unsubstituted Cp-H). <sup>13</sup>C {<sup>1</sup>H} NMR (125 MHz, DMSO-*d*<sub>6</sub>):  $\delta$  169.1 (C=O), 146.8 (triazole C or Ar-C), 145.7 (Ar-C

or triazole C), 136.7 (Ar-C), 130.9 (Ar-CH<sub>C</sub>), 125.3 (Ar-CH<sub>B</sub> or B'), 122.9 (Ar-CH<sub>B'</sub> or B), 121.2 (triazole CH), 117.0 (Ar-CH<sub>A</sub>), 76.1 (Cp-C), 70.0 (Cp-CH), 69.3 (unsubstituted Cp-CH), 68.3 (Cp-CH), 34.2 (CH<sub>2</sub>). LRMS (ESI<sup>-</sup>):  $m/z$  464.3 [M - H]<sup>-</sup>.

**N-(4-Sulfamoylphenyl) Ferrocenyl-1-carboxamide (17).** A solution of 35 (232 mg, 1.0 mmol) in DCM (5 mL) was added to a solution of 4-aminobenzenesulfonamide (1.1 equiv, 190 mg, 1.1 mmol) in DMF (0.35 mL) and pyridine (0.1 mL) and the reaction stirred for 5 days at rt. The reaction mixture was next diluted with ethyl acetate (20 mL) and washed with 2 M HCl (20 mL) and brine (2 × 20 mL). The organic fraction was dried over MgSO<sub>4</sub> and evaporated in vacuo before purification by flash chromatography (1:9 methanol:DCM) to give the title compound as an orange solid (377 mg, 0.98 mmol, 98%); mp 256–258 °C. <sup>1</sup>H NMR (500 MHz, DMSO-*d*<sub>6</sub>):  $\delta$  11.26 (s, 1H, NH), 7.58–7.61 (m, 2H, Ar-H), 6.59–6.62 (m, 2H, Ar-H), 6.08 (s, 2H, SO<sub>2</sub>NH<sub>2</sub>), 4.92 (s, 2H, Cp-H), 4.43 (s, 2H, Cp-H), 4.00 (s, 5H, unsubstituted Cp-H). <sup>13</sup>C {<sup>1</sup>H} NMR (125 MHz, DMSO-*d*<sub>6</sub>):  $\delta$  168.0 (C=O), 153.5 (Ar-C), 129.9 (Ar-CH), 112.2 (Ar-CH), 109.5 (Ar-C), 73.0 (Cp-C), 71.5 (Cp-CH), 69.5 (unsubstituted Cp-CH), 69.1 (Cp-CH). LRMS (ESI<sup>-</sup>):  $m/z$  383.2 [M - H]<sup>-</sup>.

**N-(3-Sulfamoylphenyl) Ferrocenyl-1-carboxamide (18).** The title compound was synthesized from 35 and 3-aminobenzenesulfonamide similarly to the method described for 17 (orange solid, 266 mg, 0.69 mmol, 69%); mp 183–185 °C. <sup>1</sup>H NMR (500 MHz, DMSO-*d*<sub>6</sub>):  $\delta$  9.73 (s, 1H, NH), 8.26 (s, 1H, Ar-H<sub>A</sub>), 7.95 (m, 1H, Ar-H<sub>C</sub>), 7.51 (s, 2H, Ar-H<sub>B</sub> and Ar-H<sub>B'</sub>), 7.37 (s, 2H, SO<sub>2</sub>NH<sub>2</sub>), 5.03 (apparent s, 2H, Cp-H), 4.48 (apparent s, 2H, Cp-H), 4.22 (s, 5H, unsubstituted Cp-H). <sup>13</sup>C {<sup>1</sup>H} NMR (125 MHz, DMSO-*d*<sub>6</sub>):  $\delta$  169.1 (C=O), 145.0 (Ar-C), 140.2 (Ar-C), 130.0 (Ar-CH<sub>C</sub>), 123.4 (Ar-CH<sub>B</sub> or B'), 120.6 (Ar-CH<sub>B'</sub> or B), 117.6 (Ar-CH<sub>A</sub>), 76.3 (Cp-C), 71.2 (Cp-CH), 70.0 (unsubstituted Cp-CH), 69.2 (Cp-CH). LRMS (ESI<sup>-</sup>):  $m/z$  383.5 [M - H]<sup>-</sup>.

**4-(3-Ferrocenylureido)benzenesulfonamide (19).** Compound 36 (128 mg, 0.5 mmol) was heated (100 °C) in toluene (5 mL) for 1 h then evaporated in vacuo. The resulting oil was redissolved in DCM, and a solution of 4-aminobenzenesulfonamide (1.1 equiv, 95 mg, 0.55 mmol) in DMF (1 mL) added before stirring at 50 °C for 18 h. The reaction mixture was then diluted in ethyl acetate and washed using HCl (2.0 M, 20 mL), aqueous NaHCO<sub>3</sub>(sat) (20 mL), and brine (2 × 20 mL). The organic phase was dried (MgSO<sub>4</sub>) and evaporated in vacuo before further purification by flash chromatography on silica gel (3:2 ethyl acetate:*n*-hexane). Evaporation of the eluant resulted in the isolation of the title compound as an orange solid (30 mg, 0.075 mmol, 15%); mp 268–269 °C (decomp). <sup>1</sup>H NMR (500 MHz, DMSO-*d*<sub>6</sub>):  $\delta$  8.85 (s, 1H, NH), 7.96 (s, 1H, NH), 7.71–7.72 (m, 2H, Ar-H), 7.58–7.60 (m, 2H, Ar-H), 7.17 (s, 2H, NH<sub>2</sub>), 4.53 (s, 2H, Cp-H), 4.15 (s, 4H, Cp-H), 3.97–3.98 (m, 2H, Cp-H). <sup>13</sup>C {<sup>1</sup>H} NMR (125 MHz, DMSO-*d*<sub>6</sub>):  $\delta$  152.5 (C=O), 143.0 (Ar-C), 136.6 (Ar-C), 126.7 (Ar-CH), 117.0 (Ar-CH), 96.1 (Cp-C), 68.6 (unsubstituted Cp-CH), 63.6 (Cp-CH), 60.7 (Cp-CH). LRMS (ESI<sup>-</sup>):  $m/z$  398.2 [M - H]<sup>-</sup>.

**3-(3-Ferrocenylureido)benzenesulfonamide (20).** Compound 36 (179 mg, 0.7 mmol) was heated (100 °C) in toluene (5 mL) for 1 h and then evaporated in vacuo. The resulting oil was dissolved in DCM and a solution of 3-aminobenzenesulfonamide (1.1 equiv, 132 mg, 0.77 mmol) in DMF (1 mL) added before stirring at 50 °C for 18 h. The reaction mixture was then diluted in ethyl acetate and washed using HCl (2.0 M, 20 mL), aqueous NaHCO<sub>3</sub>(sat) (20 mL), and brine (2 × 20 mL). The organic phase was dried (MgSO<sub>4</sub>) and evaporated in vacuo before further purification by flash chromatography on silica gel (3:2 ethyl acetate:*n*-hexane). Evaporation of the eluant resulted in the isolation of the title product as an orange solid (74 mg, 0.19 mmol, 26%); mp 201–202 °C. <sup>1</sup>H NMR (500 MHz, DMSO-*d*<sub>6</sub>):  $\delta$  8.78 (s, 1H, NH), 8.08 (s, 1H, Ar-H<sub>A</sub>), 7.88 (s, 1H, NH), 7.51–7.52 (m, 1H, Ar-H<sub>B</sub> or B'), 7.43–7.46 (m, 2H, Ar-H<sub>C</sub>), 7.39–7.41 (m, 1H, Ar-H<sub>B'</sub> or B), 4.54 (apparent s, 2H, Cp-H), 4.15 (s, 5H, unsubstituted Cp-H), 3.97 (s, 2H, Cp-H). <sup>13</sup>C {<sup>1</sup>H} NMR (125 MHz, DMSO-*d*<sub>6</sub>):  $\delta$  152.6 (C=O), 144.6 (Ar-C), 140.3 (Ar-C), 129.2 (Ar-CH<sub>C</sub>), 120.7 (Ar-CH<sub>B</sub> or B'), 118.4 (Ar-CH<sub>B'</sub> or B), 114.7 (Ar-CH<sub>A</sub>), 96.4 (Cp-C), 68.6

(unsubstituted Cp-CH), 63.6 (Cp-CH), 60.5 (Cp-CH). LRMS (ESI<sup>-</sup>): *m/z* 398.3 [M - H]<sup>-</sup>.

**4-(4-Phenyl-1H-1,2,3-triazol-1-yl)benzenesulfonamide (21).** The title compound was prepared from phenyl acetylene and azide 33 according to general procedure 1 and isolated as a bright-yellow solid (251 mg, 0.84 mmol, 84%); mp 284–285 °C. <sup>1</sup>H NMR (500 MHz, DMSO-*d*<sub>6</sub>): δ 9.41 (s, 1H, triazole CH), 8.17–8.19 (m, 2H, Ar-H), 8.06–8.08 (m, 2H, Ar-H), 7.95–7.97 (m, 2H, Ar-H $\alpha$ ), 7.52 (br s, 4H, Ar-H $\beta$  and SO<sub>2</sub>NH<sub>2</sub>), 7.39–7.42 (m, 1H, Ar-H $\gamma$ ). <sup>13</sup>C {<sup>1</sup>H} NMR (125 MHz, DMSO-*d*<sub>6</sub>): δ 147.6 (Ar-C), 143.8 (triazole C), 138.6 (Ar-C), 129.9 (Ar-C), 129.0 (Ar-CH $\beta$ ), 128.4 (Ar-CH $\alpha$ ), 127.5 (Ar-CH), 125.4 (Ar-CH $\gamma$ ), 120.2 (Ar-CH), 119.8 (triazole CH). LRMS (ESI<sup>-</sup>): *m/z* 299.4 [M - H]<sup>-</sup>.

**3-(4-Phenyl-1H-1,2,3-triazol-1-yl)benzenesulfonamide (22).** The title compound was prepared from phenyl acetylene and azide 34 according to general procedure 1 and isolated as bright-yellow solid (254 mg, 0.85 mmol, 85%); mp 283–284 °C. <sup>1</sup>H NMR (500 MHz, DMSO-*d*<sub>6</sub>): δ 9.43 (s, 1H, triazole CH), 8.44 (s, 1H, Ar-H<sub>A</sub>), 8.17–8.19 (m, 1H, Ar-H<sub>B or B'</sub>), 7.94–7.98 (m, 3H, Ar-H $\alpha$  and Ar-H<sub>B or B'</sub>), 7.84–7.87 (m, 1H, Ar-H<sub>C</sub>), 7.58 (br s, 2H, SO<sub>2</sub>NH<sub>2</sub>), 7.50–7.54 (m, 2H, Ar-H $\beta$ ), 7.39–7.42 (m, 1H, Ar-H $\gamma$ ). <sup>13</sup>C {<sup>1</sup>H} NMR (125 MHz, DMSO-*d*<sub>6</sub>): δ 147.6 (triazole C or Ar-C), 145.8 (Ar-C or triazole C), 136.7 (Ar-C), 130.9 (Ar-CH<sub>A</sub>), 130.0 (Ar-C), 129.0 (Ar-CH $\beta$ ), 128.4 (Ar-CH $\gamma$ ), 125.5 (Ar-CH<sub>B or B'</sub>), 125.4 (Ar-CH $\alpha$ ), 122.9 (Ar-CH<sub>B or B'</sub>), 119.8 (triazole CH), 117.0 (Ar-CH<sub>A</sub>). LRMS (ESI<sup>-</sup>): *m/z* 299.5 [M - H]<sup>-</sup>. HRMS (ESI) calcd for C<sub>14</sub>H<sub>12</sub>N<sub>4</sub>O<sub>2</sub>SH 301.0754, found 301.0739.

**4-(5-Phenyl-1H-1,2,3-triazol-1-yl)benzenesulfonamide (23).** The title compound was prepared from phenyl acetylene and azide 33 according to general procedure 2 and isolated as an off-white solid (12 mg, 0.04 mmol, 4%); mp 192–193 °C. <sup>1</sup>H NMR (500 MHz, DMSO-*d*<sub>6</sub>): δ 8.15 (s, 1H, triazole CH), 7.93–7.95 (m, 2H, Ar-H), 7.61–7.63 (m, 2H, Ar-H), 7.53 (s, 2H, SO<sub>2</sub>NH<sub>2</sub>), 7.42–7.44 (m, 3H, Ar-H $\gamma$  and Ar-H $\alpha$  or  $\beta$ ), 7.31–7.33 (m, 2H, Ar-H $\beta$  or  $\alpha$ ). <sup>13</sup>C {<sup>1</sup>H} NMR (125 MHz, DMSO-*d*<sub>6</sub>): δ 144.7 (Ar-C), 138.5 (Ar-C), 137.8 (triazole C), 133.5 (triazole CH), 129.4 (Ar-CH $\gamma$ ), 128.9 (Ar-CH $\alpha$  or  $\beta$ ), 128.6 (Ar-CH $\beta$  or  $\alpha$ ), 127.0 (Ar-CH), 126.0 (Ar-C), 125.9 (Ar-CH). LRMS (ESI<sup>-</sup>): *m/z* 299.4 [M - H]<sup>-</sup>.

**3-(5-Phenyl-1H-1,2,3-triazol-1-yl)benzenesulfonamide (24).** The title compound was prepared from phenyl acetylene and azide 34 according to general procedure 2 and isolated as an off-white solid (38 mg, 0.13 mmol, 13%); mp 189–190 °C. <sup>1</sup>H NMR (500 MHz, DMSO-*d*<sub>6</sub>): δ 8.18 (s, 1H, triazole-CH), 7.96–7.98 (m, 2H, Ar-H<sub>A</sub> and Ar-H<sub>B or B'</sub>), 7.70–7.73 (Ar-H<sub>C</sub>), 7.54–7.57 (m, 3H, Ar-H<sub>B or B'</sub> and SO<sub>2</sub>NH<sub>2</sub>), 7.43–7.44 (m, 3H, Ar-H $\alpha$ , Ar-H $\gamma$ ), 7.31–7.33 (m, 2H, Ar-H $\beta$ ). <sup>13</sup>C {<sup>1</sup>H} NMR (125 MHz, DMSO-*d*<sub>6</sub>): δ 145.5 (Ar-C), 137.8 (triazole C), 136.4 (Ar-C), 133.4 (triazole CH), 130.4 (Ar-CH<sub>C</sub>), 129.5 (Ar-CH $\gamma$ ), 128.9 (Ar-CH $\alpha$ ), 128.6 (Ar-CH<sub>B or B'</sub>), 128.5 (Ar-CH $\beta$ ), 126.5 (Ar-CH<sub>B or B'</sub>), 125.9 (Ar-C), 122.6 (Ar-CH<sub>A</sub>). LRMS (ESI<sup>-</sup>): *m/z* 299.4 [M - H]<sup>-</sup>. HRMS (ESI) calcd for C<sub>14</sub>H<sub>12</sub>N<sub>4</sub>O<sub>2</sub>SH 301.0754, found 301.0740.

**4-(1H-1,2,3-Triazol-1-yl)benzenesulfonamide (25).** The title compound was prepared from ethynyltrimethylsilane and azide 33 according to general procedure 1, followed by reaction with TBAF (1.0 M in THF, 5 mL) at rt for 2 h. The solvent was evaporated in vacuo and the residue purified on a silica gel column (1:1 ethyl acetate:*n*-hexane) to give a pale-yellow solid (122 mg, 0.54 mmol, 88%); mp 187–189 °C. <sup>1</sup>H NMR (500 MHz, DMSO-*d*<sub>6</sub>): δ 8.93 (s, 1H, triazole CH<sub>5</sub>), 8.13–8.15 (m, 2H, Ar-H), 8.02–8.04 (m, 3H, triazole CH<sub>4</sub>, Ar-H), 7.51 (s, 2H, SO<sub>2</sub>NH<sub>2</sub>). <sup>13</sup>C {<sup>1</sup>H} NMR (125 MHz, DMSO-*d*<sub>6</sub>): δ 143.8 (Ar-C), 138.6 (Ar-C), 134.7 (triazole CH<sub>4</sub>), 127.4 (Ar-CH), 123.5 (triazole CH<sub>5</sub>), 120.3 (Ar-CH). LRMS (ESI<sup>-</sup>): *m/z* 223.4 [M - H]<sup>-</sup>. HRMS (ESI) calcd for C<sub>8</sub>H<sub>9</sub>N<sub>4</sub>O<sub>2</sub>SH 225.0437, found 225.0440.

**3-(1H-1,2,3-Triazol-1-yl)benzenesulfonamide (26).** The title compound was prepared from ethynyltrimethylsilane and azide 34 according to general procedure 1 and isolated as a pale-yellow solid (83 mg, 0.37 mmol, 37%); mp 172–173 °C. <sup>1</sup>H NMR (500 MHz, DMSO-*d*<sub>6</sub>): δ 8.92 (s, 1H, triazole CH<sub>5</sub>), 8.39 (s, 1H, Ar-H<sub>A</sub>), 8.13–8.14 (m, 1H, Ar-H<sub>B or B'</sub>), 8.03 (s, 1H, triazole CH<sub>4</sub>), 7.92–7.93 (m,

1H, Ar-H<sub>B or B'</sub>), 7.80–7.84 (m, 1H, Ar-H<sub>C</sub>), 7.56 (s, 2H, SO<sub>2</sub>NH<sub>2</sub>). <sup>13</sup>C {<sup>1</sup>H} NMR (125 MHz, DMSO-*d*<sub>6</sub>): δ 145.7 (Ar-C), 136.8 (Ar-C), 134.7 (triazole CH<sub>4</sub>), 130.8 (Ar-CH<sub>C</sub>), 125.4 (Ar-CH<sub>B or B'</sub>), 123.5 (triazole CH<sub>5</sub>), 123.1 (Ar-CH<sub>B or B'</sub>), 117.3 (Ar-CH<sub>A</sub>). LRMS (ESI<sup>-</sup>): *m/z* 447.4 [2M - H]<sup>-</sup>. HRMS (ESI) calcd for C<sub>8</sub>H<sub>9</sub>N<sub>4</sub>O<sub>2</sub>SH 225.0437, found 225.0436.

**Prop-2-ynyl Ferrocenyl-1-carboxylate (29).** The title compound was prepared from propargyl alcohol according to general procedure 3 and isolated as an orange solid (250 mg, 0.93 mmol, 93%); mp 83.5–85.0 °C. <sup>1</sup>H NMR (500 MHz, DMSO-*d*<sub>6</sub>): δ 4.79 (s, 2H, Cp-CH), 4.52 (s, 2H, Cp-CH), 4.42 (br s, 2H, CH<sub>2</sub>), 4.27 (s, 5H, unsubstituted Cp-CH), C $\equiv$ CH not detected. <sup>13</sup>C {<sup>1</sup>H} NMR (125 MHz, DMSO-*d*<sub>6</sub>): δ 170.5 (C=O), 79.2 (C $\equiv$ CH), 77.3 (Cp-C), 71.7 (Cp-CH), 69.8 (Cp-CH), 69.6 (unsubstituted Cp-CH), 69.5 (C $\equiv$ CH), 51.3 (CH<sub>2</sub>).

**But-3-ynyl Ferrocenyl-1-carboxylate (30).** The title compound was prepared from 1-butynyl alcohol according to general procedure 3 and isolated as an orange solid (272 mg, 0.96 mmol, 96%); mp 67–68 °C. <sup>1</sup>H NMR (500 MHz, DMSO-*d*<sub>6</sub>): δ 4.75 (s, 2H, Cp-CH), 4.49 (s, 2H, Cp-CH), 4.22–4.25 (m, 7H, unsubstituted Cp-CH,  $\alpha$ CH<sub>2</sub>), 2.92 (br s, 2H,  $\beta$ CH<sub>2</sub>), C $\equiv$ CH not detected. <sup>13</sup>C {<sup>1</sup>H} NMR (125 MHz, DMSO-*d*<sub>6</sub>): δ 170.4 (C=O), 80.9 (C $\equiv$ CH), 72.2 (Cp-C), 71.3 (Cp-CH), 70.3 (C $\equiv$ CH), 69.6 (Cp-CH), 69.5 (unsubstituted Cp-CH), 61.5 ( $\alpha$ CH<sub>2</sub>), 18.4 ( $\beta$ CH<sub>2</sub>).

**Pent-4-ynyl Ferrocenyl-1-carboxylate (31).** The title compound was prepared from 4-pentynyl alcohol according to general procedure 3 and isolated as an orange solid (293 mg, 0.99 mmol, 99%); mp 84–85 °C. <sup>1</sup>H NMR (500 MHz, DMSO-*d*<sub>6</sub>): δ 4.76 (s, 2H, Cp-CH), 4.49 (s, 2H, Cp-CH), 4.20–4.23 (m, 7H, unsubstituted Cp-CH,  $\alpha$ CH<sub>2</sub>), 2.35 (br s, 2H,  $\gamma$ CH<sub>2</sub>), 1.84–1.86 (m, 3H,  $\beta$ CH<sub>2</sub>, C $\equiv$ CH). <sup>13</sup>C {<sup>1</sup>H} NMR (125 MHz, DMSO-*d*<sub>6</sub>): δ 170.5 (C=O), 83.4 (C $\equiv$ CH), 71.7 (Cp-C), 71.3 (Cp-CH), 70.7 (C $\equiv$ CH), 69.7 (Cp-CH), 69.5 (unsubstituted Cp-CH), 62.2 ( $\alpha$ CH<sub>2</sub>), 27.2 ( $\beta$ CH<sub>2</sub>), 18.4 ( $\gamma$ CH<sub>2</sub>).

**Prop-2-ynyl Ferrocenyl-1-carboxamide (32).** The title compound was prepared from propargyl amine according to a modified general procedure 3 (omit -4-dimethylamino pyridine, THF as solvent, purification by silica gel chromatography (1:9 methanol: dichloromethane)) and isolated as an orange solid (281 mg, 1.05 mmol, 70%); mp 192.9–197.1 °C. <sup>1</sup>H NMR (500 MHz, DMSO-*d*<sub>6</sub>): δ 8.20 (br s, 1H, NH), 4.81 (s, 2H, Cp-CH), 4.35 (s, 2H, Cp-CH), 4.19 (s, 5H, unsubstituted Cp-CH), 3.96 (d, <sup>3</sup>J<sub>CH-NH</sub> = 6 Hz, 2H, CH<sub>2</sub>), C $\equiv$ CH not detected. <sup>13</sup>C {<sup>1</sup>H} NMR (125 MHz, DMSO-*d*<sub>6</sub>): δ 168.9 (C=O), 82.1 (C $\equiv$ CH), 75.6 (C $\equiv$ CH), 72.3 (Cp-C), 70.1 (Cp-CH), 69.2 (unsubstituted Cp-CH), 68.2 (Cp-CH), 27.9 (CH<sub>2</sub>).

**3-Azidobenzenesulfonamide (34).** To a suspension of 3-aminobenzenesulfonamide (5.0 g, 29 mmol, 1.0 equiv) in acetonitrile (50 mL) at 0 °C was added dropwise *t*-butyl nitrite (5.0 mL, 1.5 equiv), followed by azidotrimethylsilane (3.4 mL, 1.2 equiv). The resulting bright-yellow solution was stirred at rt for 16 h. The reaction mixture was reduced to dryness in vacuo and the remaining residue dissolved in EtOAc (50 mL) and washed with brine (50 mL). The aqueous phase was back-extracted with EtOAc (50 mL), the organic fractions were combined and again washed with brine (2  $\times$  50 mL), dried (MgSO<sub>4</sub>), and the solvent volume reduced (ca. 20 mL). The product was precipitated by addition of *n*-hexane, collected by vacuum filtration and washed with *n*-hexane to produce a pale-yellow solid (3.7 g, 19 mmol, 64%); mp 143–144 °C. <sup>1</sup>H NMR (500 MHz, DMSO-*d*<sub>6</sub>): δ 7.59–7.63 (m, 2H, Ar-H<sub>A</sub>, Ar-H<sub>B or B'</sub>), 7.51–7.52 (m, 1H, Ar-H<sub>B or B'</sub>), 7.80–7.84 (m, 1H, Ar-H<sub>C</sub>), 7.45 (s, 2H, SO<sub>2</sub>NH<sub>2</sub>). <sup>13</sup>C {<sup>1</sup>H} NMR (125 MHz, DMSO-*d*<sub>6</sub>): δ 145.8 (Ar-C), 140.3 (Ar-C), 130.8 (Ar-CH<sub>A</sub>), 122.4 (Ar-CH<sub>B or B'</sub>), 122.0 (Ar-CH<sub>B or B'</sub>), 116.0 (Ar-CH<sub>C</sub>). LRMS (ESI<sup>-</sup>): *m/z* 197.3 [M - H]<sup>-</sup>.

**Ferrocenylaclyazide (36).** A solution of 35 (1.0 g, 4.3 mmol) in THF (2 mL) was combined with a solution of sodium azide (4.5 equiv, 1.26 g, 19.4 mmol) in water (10 mL). The reaction mixture was stirred for 3 h at rt, after which a red precipitate had formed. The precipitate was collected by vacuum filtration, washed with deionized water, and dried to give the crude product (414 mg, 1.6 mmol, 37%). Product was used without further purification; mp 99–100 °C. <sup>1</sup>H

NMR (500 MHz,  $\text{CDCl}_3$ ):  $\delta$  4.80 (s, 2H, Cp-H), 4.49 (s, 2H, Cp-H), 4.24 (s, 5H, unsubstituted Cp-H). IR (KBr Disc):  $\nu$  2152 (s,  $\text{N}_3$ ), 1678 (s, C=O)  $\text{cm}^{-1}$ .

**Partition Coefficient Determinations.** Partition coefficients (Log  $D$ ) were determined chromatographically by comparing their retention properties to a set of standard compounds with known partition coefficients using a modification of a previously published method.<sup>20</sup> Data were collected using a Waters 2795 HPLC instrument with a Waters 2487 dual channel UV detector with a Phenomenex Synergi Hydro-RP 4  $\mu\text{m}$  (30 mm  $\times$  2 mm) column. The mobile phase was aqueous buffer (50 mM ammonium acetate, pH 7.4) and acetonitrile with an acetonitrile gradient of 0–100% over 10 min. Compound elution was monitored at 220 and 254 nm. Log  $D$  values were also determined using a shake flask method, in which a stock solution of the test compound was first prepared in octanol at a concentration of 10 mg/mL and diluted with octanol to a concentration of 2 mg/mL. The diluted octanol solution was mixed with an equal volume of aqueous buffer, gently vortexed, and then incubated at 25 °C for 24–96 h. Samples were periodically withdrawn and centrifuged (3 min  $\times$  10000 rpm), after which aliquots (150  $\mu\text{L}$ ) were taken from each phase. The aliquots were further diluted and then analyzed by LCMS to determine the compound concentration in each phase.

**Permeability Measurements.** Caco-2 cells (passage 32) were seeded onto 0.3  $\text{cm}^2$  polycarbonate filter transwells at a density of 60000 cells/well. Confluent cell monolayers were obtained 21 days postseeding. The integrity of the cell monolayers was determined by measuring the transepithelial electrical resistance (TEER), and only monolayers with TEER values of  $>270 \Omega \cdot \text{cm}^2$  were utilized. The permeability of  $^{14}\text{C}$ -mannitol and  $^3\text{H}$ -propranolol (low and high permeability markers, respectively) was also assessed using a subset of wells from the same batch as those used to assess the test compounds. Permeability experiments were performed using Hank's balanced salt solution containing 20 mM HEPES (pH 7.4) in both the apical and basolateral chambers, and permeability was assessed in the apical to basolateral (A–B) direction using an initial donor solution concentration of 10  $\mu\text{M}$  for 5, 2.5  $\mu\text{M}$  for 21, 20  $\mu\text{M}$  for 37, and 0.7  $\mu\text{M}$  for 1. Test compound solubility in the transport buffer was confirmed prior to the experiment. Compound flux was determined over 90 min with samples taken from the acceptor chamber at 5, 15, 30, 45, 60, and 90 min. At each sample time, the volume of acceptor solution removed was replaced with blank transport buffer and acceptor concentrations were corrected for this dilution. Donor samples were taken at the start and completion of the experiment. The amount of compound transported was quantitated by LC-MS or by liquid scintillation counting.

**Solubility Measurements.** The solubility in aqueous buffers was determined using either a kinetic screening method or an equilibrium method. For the kinetic method, compound in DMSO (10 mg/mL) was spiked into either pH 6.5 phosphate buffer or 0.01 M HCl (approximate pH 2.0), with the final DMSO concentration being 1%. Samples were then analyzed via nephelometry to determine a solubility range.<sup>22</sup> Equilibrium solubility measurements were conducted by adding media (water, pH 2 or pH 6.5 buffers) to preweighed compound in screw cap polypropylene tubes, followed by vortexing and incubating at 25 °C for 24 h. Additional compound was added if compounds were completely dissolved to ensure that the solution was saturated. Sampling was performed after 1, 4, and 24 h by centrifuging (3 min  $\times$  10000 rpm) and then removing aliquots of the supernatant for analysis by LCMS.

**In Vitro Metabolic Stability.** Human liver microsomes (BD Gentest, Discovery Labware Inc., Woburn, Massachusetts) were suspended in 0.1 M phosphate buffer (pH 7.4) at a final protein concentration of 0.4 mg/mL and incubated with compounds (1  $\mu\text{M}$ ) at 37 °C. An NADPH-regenerating system (1 mg/mL NADP, 1 mg/mL glucose-6-phosphate, 1 U/mL glucose-6-phosphate dehydrogenase) and  $\text{MgCl}_2$  (0.67 mg/mL) was added to initiate the metabolic reactions, which were subsequently quenched with ice-cold acetonitrile at time points ranging from 0 to 60 min. Samples were also incubated in the absence of cofactor to monitor for noncytochrome P450-

mediated metabolism in the microsomal matrix. Samples were then centrifuged and the concentration of parent compound remaining in the supernatant monitored by LCMS. The first-order rate constant for substrate depletion was determined by fitting the data to an exponential decay function and these values were used to calculate the in vitro intrinsic clearance ( $\text{CL}_{\text{int}}$ ) and the predicted in vivo intrinsic clearance value ( $\text{CL}_{\text{int vivo}}$ ) as previously described.<sup>23</sup> The predicted in vivo hepatic extraction ratio ( $E_h$ ) was calculated using the following relationship:  $E_h = \text{CL}_{\text{int vivo}} / (Q + \text{CL}_{\text{int vivo}})$  where  $Q$  is liver blood flow (20.7 mL/min/kg).

**LCMS Analysis.** LCMS analysis was conducted using a Waters Acquity HPLC system coupled to either a Waters Xevo or a Waters Quattro Ultima Premier mass spectrometer operated under positive ion MS-MS conditions. The column was a Supelco Ascentis Express Amide (2.7  $\mu\text{m}$ , 50 mm  $\times$  2.1 mm i.d.) maintained at a column temperature of 40 °C. HPLC analysis was performed using a mobile phase consisting of water and methanol containing 0.005% ammonium formate at a flow rate of 0.4 mL/min, and separation was achieved under gradient conditions varying the methanol content from 2 to 95% followed by equilibration to the starting conditions. Processed samples were maintained in the autosampler at a temperature of 10 °C and 5  $\mu\text{L}$  were injected onto the column. The conditions described led to the elution of 35, 21, 1, and 5 after 1.84, 2.22, 2.41, and 2.41 min, respectively. Compounds were quantified by comparison to calibration curves prepared in the sample matrix.

## ■ ASSOCIATED CONTENT

### 📄 Supporting Information

$^1\text{H}$  NMR spectra of compounds 5–26. This material is available free of charge via the Internet at <http://pubs.acs.org>.

## ■ AUTHOR INFORMATION

### Corresponding Author

\*For S.-A.P.: phone, +61 7 3735 7825; fax, +61 7 3735 7656; E-mail, [s.poulsen@griffith.edu.au](mailto:s.poulsen@griffith.edu.au). For C.T.S.: phone, +39 55 457 3005; fax, +39 55 457 3385; E-mail, [claudiu.supuran@unifi.it](mailto:claudiu.supuran@unifi.it).

### Notes

The authors declare no competing financial interest.

## ■ ACKNOWLEDGMENTS

This research was financed by the Australian Research Council (DP110100071), Australian Government (Student Scholarship to A.J.S.) and by a grant of the 7th FP of EU (Metoxia). The technical assistance of Ms Thao Pham and Dr Eileen Ryan are gratefully acknowledged.

## ■ ABBREVIATIONS USED

CA, carbonic anhydrase; ZBG, zinc binding group; 1,3-DCR, 1,3-dipolar cycloaddition reaction; SPR, structure–property relationship; CuAAC, copper-catalyzed azide–alkyne cycloaddition; RuAAC, ruthenium-catalyzed azide–alkyne cycloaddition; ADME, adsorption distribution metabolism excretion;  $\text{CL}_{\text{int}}$ , in vitro intrinsic clearance;  $\text{CL}_{\text{int vivo}}$ , in vivo intrinsic clearance;  $E_h$ , in vivo hepatic extraction ratio

## ■ REFERENCES

- (1) (a) Hartinger, C.; Dyson, P. J. Bioorganometallic chemistry: from teaching paradigms to medicinal applications. *Chem. Soc. Rev.* **2009**, *38*, 391–401. (b) Gasser, G.; Ott, I.; Metzler-Nolte, N. Organometallic Anticancer Compounds. *J. Med. Chem.* **2011**, *54*, 3–25.
- (2) Rausch, M. D.; Fischer, E. O.; Grubert, H. The Aromatic Reactivity of Ferrocene, Ruthenocene and Osmocene. *J. Am. Chem. Soc.* **1960**, *82* (1), 76–82.
- (3) van Staveren, D. R.; Metzler-Nolte, N. Bioorganometallic Chemistry of Ferrocene. *Chem. Rev.* **2004**, *104* (12), 5931–5986.

(4) Köpf-Maier, P.; Köpf, H.; Neuse, E. W. Ferrocenium salts; the first antineoplastic iron compounds. *Angew. Chem., Int. Ed. Engl.* **1984**, *23*, 456–457.

(5) Top, S.; Vessieres, A.; Leclercq, G.; Quivy, J.; Tang, J.; Vaissermann, J.; Huche, M.; Jaouen, G. Synthesis, Biochemical Properties and Molecular Modelling Studies of Organometallic Specific Estrogen Receptor Modulators (SERMs), the Ferrocifens and Hydroxyferrocifens: Evidence for an Antiproliferative Effect of Hydroxyferrocifens on both Hormone-Dependent and Hormone-Independent Breast Cancer Cell Lines. *Chem.—Eur. J.* **2003**, *9*, 5223–5236.

(6) Dive, D.; Biot, C. Ferrocene Conjugates of Chloroquine and other Antimalarials: The Development of Ferroquine, a New Antimalarial. *ChemMedChem* **2008**, *3* (3), 383–391.

(7) (a) Salmon, A. J.; Williams, M. L.; Innocenti, A.; Vullo, D.; Supuran, C. T.; Poulsen, S.-A. Inhibition of carbonic anhydrase isozymes I, II and IX with benzenesulfonamides containing an organometallic moiety. *Bioorg. Med. Chem. Lett.* **2007**, *17* (18), 5032–5035. (b) Schobert, R.; Seibt, S.; Mahal, K.; Ahmad, A.; Biersack, B.; Effenberger-Neidnicht, K.; Padhye, S.; Sarkar, F. H.; Muelle, T. Cancer Selective Metalloenediarylates of the Fungal Cytotoxin Illudin M. *J. Med. Chem.* **2011**, *54*, 6177–6182.

(8) Krishnamurthy, V. M.; Kaufman, G. K.; Urbach, A. R.; Gitlin, I.; Gudiksen, K. L.; Weibel, D. B.; Whitesides, G. M. Carbonic Anhydrase as a Model for Biophysical and Physical–Organic Studies of Proteins and Protein–Ligand Binding. *Chem. Rev.* **2008**, *108* (3), 946–1051.

(9) (a) Chiche, J.; Ilc, K.; Laferriere, J.; Trotter, E.; Dayan, F.; Mazure, N. M.; Brahimi-Horn, M. C.; Pouyssegur, J. Hypoxia-Inducible Carbonic Anhydrase IX and XII Promote Tumor Cell Growth by Counteracting Acidosis through the Regulation of the Intracellular pH. *Cancer Res.* **2009**, *69* (1), 358–368. (b) Swietach, P.; Vaughan-Jones, R.; Harris, A. Regulation of tumor pH and the role of carbonic anhydrase 9. *Cancer Metastasis Rev.* **2007**, *26* (2), 299–310. (c) Wykoff, C. C.; Beasley, N. J.; Watson, P. H.; Turner, K. J.; Pastorek, J.; Sibtain, A.; Wilson, G. D.; Turley, H.; Talks, K. L.; Maxwell, P. H.; Pugh, C. W.; Ratcliffe, P. J.; Harris, A. L. Hypoxia-Inducible Expression of Tumor-Associated Carbonic Anhydrases. *Cancer Res.* **2000**, *60* (24), 7075–7083.

(10) Neri, D.; Supuran, C. T. Interfering with pH regulation in tumours as a therapeutic strategy. *Nature Rev. Drug Discovery* **2011**, *10*, 767–777.

(11) (a) Morris, J. C.; Chiche, J.; Grellier, C.; Lopez, M.; Bornaghi, L. F.; Maresca, A.; Supuran, C. T.; Pouyssegur, J.; Poulsen, S.-A. Targeting Hypoxic Tumor Cell Viability with Carbohydrate-Based Carbonic Anhydrase IX and XII Inhibitors. *J. Med. Chem.* **2011**, *54*, 6905–6918. (b) Lou, Y.; McDonald, P. C.; Oloumi, A.; Chia, S.; Ostlund, C.; Ahmadi, A.; Kyle, A.; auf dem Keller, U.; Leung, S.; Huntsman, D.; Clarke, B.; Sutherland, B. W.; Waterhouse, D.; Bally, M.; Roskelley, C.; Overall, C. M.; Minchinton, A.; Pacchiano, F.; Carta, F.; Scozzafava, A.; Touisni, N.; Winum, J.-Y.; Supuran, C. T.; Dedhar, S. Targeting Tumor Hypoxia: Suppression of Breast Tumor Growth and Metastasis by Novel Carbonic Anhydrase IX Inhibitors. *Cancer Res.* **2011**, *71*, 3364–3376.

(12) Salmon, A. J.; Williams, M. L.; Hofmann, A.; Poulsen, S.-A. Protein crystal structures with ferrocene and ruthenocene-based enzyme inhibitors. *Chem. Commun.* **2012**, *48* (17), 2328–2330.

(13) (a) Can, D.; Spingler, B.; Schmutz, P.; Mendes, F.; Raposinho, P.; Fernandes, C.; Carta, F.; Innocenti, A.; Santos, I.; Supuran, C.; Alberto, R. [(Cp-R)M(CO)<sub>3</sub>] (M = Re or 99mTc) Arylsulfonamide, Arylsulfamide, and Arylsulfamate Conjugates for Selective Targeting of Human Carbonic Anhydrase IX. *Angew. Chem., Int. Ed. Engl.* **2012**, *51*, 3354–3357. (b) Monnard, F. W.; Heinisch, T.; Nogueira, E. S.; Schirmer, T.; Ward, T. R. Human Carbonic Anhydrase II as a host for piano-stool complexes bearing a sulfonamide anchor. *Chem. Commun.* **2011**, *47*, 8238–8240.

(14) Supuran, C. T. Carbonic anhydrases: novel therapeutic applications for inhibitors and activators. *Nature Rev. Drug Discovery* **2008**, *7* (2), 168–181.

(15) (a) Lopez, M.; Salmon, A. J.; Supuran, C. T.; Poulsen, S.-A. Carbonic anhydrase inhibitors developed through “click tailing”. *Curr. Pharm. Des.* **2010**, *16* (29), 3277–3287. (b) Winum, J.-Y.; Poulsen, S.-A.; Supuran, C. T. Therapeutic applications of glycosidic carbonic anhydrase inhibitors. *Med. Res. Rev.* **2009**, *29* (3), 419–435.

(16) (a) Salmon, A. J.; Williams, M. L.; Maresca, A.; Supuran, C. T.; Poulsen, S.-A. Synthesis of glycoconjugate carbonic anhydrase inhibitors by ruthenium-catalysed azide-alkyne 1,3-dipolar cycloaddition. *Bioorg. Med. Chem. Lett.* **2011**, *21*, 6058–6061. (b) Singer, M.; Lopez, M.; Bornaghi, L. F.; Innocenti, A.; Vullo, D.; Supuran, C. T.; Poulsen, S.-A. Inhibition of carbonic anhydrase isozymes with benzene sulfonamides incorporating thio, sulfinyl and sulfonyl glycoside moieties. *Bioorg. Med. Chem. Lett.* **2009**, *19* (8), 2273–2276. (c) Wilkinson, B. L.; Innocenti, A.; Vullo, D.; Supuran, C. T.; Poulsen, S.-A. Inhibition of Carbonic Anhydrases with Glycosyltriazole Benzene Sulfonamides. *J. Med. Chem.* **2008**, *51* (6), 1945–1953. (d) Wilkinson, B. L.; Bornaghi, L. F.; Houston, T. A.; Innocenti, A.; Vullo, D.; Supuran, C. T.; Poulsen, S.-A. Carbonic Anhydrase Inhibitors: Inhibition of Isozymes I, II, and IX with Triazole-Linked O-Glycosides of Benzene Sulfonamides. *J. Med. Chem.* **2007**, *50* (7), 1651–1657. (e) Wilkinson, B. L.; Bornaghi, L. F.; Houston, T. A.; Innocenti, A.; Vullo, D.; Supuran, C. T.; Poulsen, S.-A. Inhibition of membrane-associated carbonic anhydrase isozymes IX, XII and XIV with a library of glycoconjugate benzenesulfonamides. *Bioorg. Med. Chem. Lett.* **2007**, *17* (4), 987–992. (f) Wilkinson, B. L.; Bornaghi, L. F.; Houston, T. A.; Innocenti, A.; Supuran, C. T.; Poulsen, S.-A. A novel class of carbonic anhydrase inhibitors: Glycoconjugate benzene sulfonamides prepared by “click-tailing”. *J. Med. Chem.* **2006**, *49* (22), 6539–6548.

(17) Galow, T. H.; Rodrigo, J.; Cleary, K.; Cooke, G.; Rotello, V. M. Fluorocarbonylferrocene. A versatile intermediate for ferrocene esters and amides. *J. Org. Chem.* **1999**, *64* (10), 3745–3746.

(18) Das, J.; Patil, S. N.; Awasthi, R.; Narasimhulu, C. P.; Trehan, S. An easy access to aryl azides from aryl amines under neutral conditions. *Synthesis* **2005**, *11*, 1801–1806.

(19) Walters, W. P.; Green, J.; Weiss, J. R.; Murcko, M. A. What Do Medicinal Chemists Actually Make? A 50-Year Retrospective. *J. Med. Chem.* **2011**, *54* (19), 6405–6416.

(20) Lombardo, F.; Shalava, M. Y.; Tupper, K. A.; Gao, F. ElogDoct: A Tool for Lipophilicity Determination in Drug Discovery. 2. Basic and Neutral Compounds. *J. Med. Chem.* **2001**, *44*, 2490–2497.

(21) Abraham, M. H.; Benjelloun-Dakhama, N.; Gola, J. M. R.; Acree, W. E., Jr.; Cain, W. S.; Cometto-Muniz, J. E. Solvation descriptors for ferrocene, and the estimation of some physicochemical and biochemical properties. *New J. Chem.* **2000**, *24*, 825–829.

(22) Bevan, C. D.; Lloyd, R. S. A High-Throughput Screening Method for the Determination of Aqueous Drug Solubility Using Laser Nephelometry in Microtiter Plates. *Anal. Chem.* **2000**, *72* (8), 1781–1787.

(23) Obach, R. S. Prediction of Human Clearance of Twenty-Nine Drugs from Hepatic Microsomal Intrinsic Clearance Data: An Examination of In Vitro Half-Life Approach and Nonspecific Binding to Microsomes. *Drug Metab. Dispos.* **1999**, *27*, 1350–1359.